NUCLEAR STRUCTURE STUDIES OF ^{142}PR

NUCLEAR STRUCTURE STUDIES OF ^{142}Pr

By

KONRAD ANTON ANIOL, B.SC.

A Thesis

Submitted to the School of Graduate Studies

in Partial Fulfilment of the Requirements

for the Degree

Master of Science

McMaster University

January 1973

MASTER OF SCIENCE (1973)   McMASTER UNIVERSITY

(Physics)   Hamilton, Ontario.

TITLE: Nuclear Structure Studies of ^{142}Praseodymium

AUTHOR: Konrad Anton Aniol, B.Sc.   (University of Illinois)

SUPERVISOR: Professor R.G. Summers-Gill

NUMBER OF PAGES: vii,93

ABSTRACT:

      The independent quasi particle model of nuclear excited states has successfully been applied by previous authors to the N = 83 nuclei ^{140}La and ^{142}Pr. In both these nuclei configuration mixing between the $(\pi 1g_{7/2})2f_{7/2})$ and $(\pi 2d_{5/2})2f_{7/2})$ configurations is expected to produce 14 negative parity states with spins 0,1,1,2,2,3,3,4,4,5,5,6,6,7. In the case of ^{140}La all fourteen states have been identified among the low lying excitations (below 600 kev). In ^{142}Pr previous research had placed 10 of the expected low lying states, and all of these were located below 200 kev.

      In our research, using data from ^{139}La(d,n) gamma-gamma coincidence, from ^{141}Pr(d,p), and ^{144}Nd(d,d), we were able to suggest the locations of three new nuclear levels in ^{142}Pr, two of which we believe to be the 6$^-$ and 7$^-$ spin states not seen by previous investigators. The results are encouraging because these two levels are found at approximately the same excitation energy as the corresponding states in ^{140}La, and one hopes, therefore, that the similarity in level structure between these two nuclei can be explained

by a neutron-proton interaction common to both nuclei.
The three new states which we are suggesting are,

energy(kev)	spin
89.739(.006)	6^-
358.11(.10)	7^-
910.97(.30)	

ACKNOWLEDGEMENTS:

Table of Contents

List of Figures

List of Tables

To Kathye

Introduction

Attempts at determining the nature of the forces
that give rise to the various phenomena observed in
Nature, have often compelled physicists to investigate
the structures of the systems in which these forces are
operant. For example, by studying the movements of the
members of the solar system, Newton was led to the formulation
of the gravitational force.

When one considers the atomic nucleus, an immediately
striking feature of this system is the confinement of many
protons to incredibly small volumes. In ^{142}Praseodymium,
for example, 59 protons are confined within a roughly
spherical volume of radius 7.5 fm(1 fm = 1 femtometer =
10^{-13} cm). Since electrons do not exist within the nucleus
as components of the nuclear system, and since the only known
constituents of the nucleus are neutrons and protons, the
tremendously repulsive coulomb potential associated with
the protons is not masked. This indicates that there is another
force, which we call the nuclear force, that binds the
nucleons into the nucleus. By scattering protons off protons
and neutrons, and by comparing mirror nuclei, it has been
determined that the proton-proton, proton-neutron, and
neutron-neutron interactions are the same, at least for
the singlet (I = 0) state.

Since we will be discussing nuclear structure, it
would be helpful if we fixed in our minds what we mean by
structure. For example, the structure of the solar system
at any given moment in time can be described by giving the
locations and velocities of all its components at that
moment. In short, we can say that the structure of the
solar system at any given moment is described by the

1

configuration its components assume at that moment.
Analogously, nuclear structure can be discussed by describing
the configurations which the nuclear components, i.e., the
protons and neutrons, can assume. Unlike the solar system,
which can take on continuously different configurations
(e.g., different planetary orbits), the nucleus can only
take on discretely different configurations. Sometimes we
can not say exactly which configuration the nucleus is in,
so we assign probabilities to various possible configuartions,
and the weighted sum of these possible configurations we
refer to as a state. For example, suppose we have a nucleus
of 2 protons and 2 neutrons and that there are two possible
configurations as diagrammed below

configuration $|A\rangle$
configuration $|B\rangle$
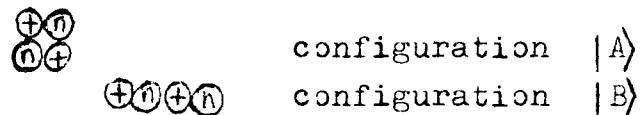
The probability that the nucleus is in configuration $|A\rangle$ is,
say, 60%. Then the probability that it is in configuration
$|B\rangle$ is 40%. Let us refer to a state by " $|State\rangle$ ". Then
we could say in general that

$$|State\rangle = a|A\rangle + b|B\rangle$$

where

a^2 = probability that the nucleus is in configuration
$|A\rangle$

b^2 = probability that the nucleus is in configuration
$|B\rangle$

If either a or b happen to be zero, then the state is the
same as the configuration.

We can not observe nuclear states directly, as we
can the "states" of the solar system. But we can infer about
their possible configurations by observing the nucleus as
it changes from state to state. For example, suppose we have

two states,using the configurations above.

$$|\text{State } 1\rangle \quad = \quad \begin{array}{cc} \oplus \ ⓝ \\ ⓝ \ \oplus \end{array} \quad = \quad |A\rangle$$

$$|\text{State } 2\rangle \quad = \quad \oplus ⓝ \oplus ⓝ \quad = \quad |B\rangle$$

and suppose the protons and neutrons rearrange themselves
from configuration $|A\rangle$ to configuration $|B\rangle$, that is,
the nucleus goes from $|\text{State } 1\rangle$ to $|\text{State } 2\rangle$.

$$|\text{State } 1\rangle \longrightarrow |\text{State } 2\rangle \quad + \quad \text{gamma ray}$$

$$\begin{array}{cc} \oplus ⓝ \\ ⓝ \oplus \end{array} \longrightarrow \oplus ⓝ \oplus ⓝ \quad + \quad \text{gamma ray}$$
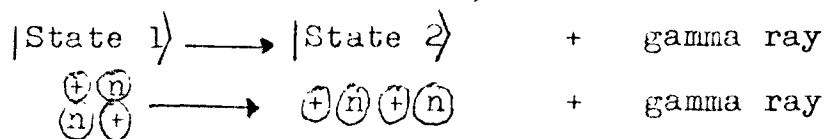
If the internal energy of $|\text{State } 1\rangle$ is greater than that of
$|\text{State } 2\rangle$, then the transition between states will release
a gamma ray whose energy is equal to the difference in
energy between the states. By measuring the gamma ray energies
we can , at least, determine the differences in energy between
various nuclear states. We can also obtain information about
the states by measuring other properties of the gamma rays;
e.g., do the gamma rays have a preferred direction of emission?
We have other ways of observing the structure of the states ,
and these will be discussed in the chapter on the experimental
work, chapter 4.

It should be remembered that the configurations are
produced by the interactions between the nucleons. Thus, by
determining the configurations we hope to determine the
inter nucleon forces. We believe that nuclei with 83 neutrons
should be relatively simple because 82 of the neutrons are
believed to form a relatively inert core, leaving only one
neutron to interact with the protons in the system. In
^{142}Pr we have 59 protons. 50 of these protons form a relatively
inert core, so in all, we have to consider only the interactions
of the 9 protons and the one neutron.

The remainder of this thesis consists of; chapter 1,
in which we discuss theoretical aspects of nuclear structure

in the N = 83 region, chapter 2 which discusses previous
research on ^{142}Pr, chapter 3 which describes the coincidence
method which is the chief experimental technique used in
placing 3 newly suggested energy levels in ^{142}Pr, then
chapter 4 which describes the experiments and the data we
obtained from them, and finally chapter 5 in which we discuss
the data and attempt to justify placing three new nuclear
energy levels at 89.739(.006) kev, 358.11(.10) kev, and
910.97 (.30) kev. We also consider in the last chapter the
implication of the data on the structures and possible
configurations of these three energy levels.

Chapter 1

Brief Theoretical Background

Overview:

  Theoretical aspects of the $N = 83$ nuclei
are considered. The independent quasi particle
model is employed by Kern et al.(1967) on
^{140}La and is found to satisfactorily
describe the low lying excitations. For
^{142}Pr the model predicts 14 low lying
(less than about 600 kev) states of spins
 and parities

$$0^-,1^-,2^-,3^-,4^-,5^-,6^-,7^-$$
$$1^-,2^-,3^-,4^-,5^-,6^- \quad .$$

BRIEF THEORETICAL BACKGROUND

The predictions of the properties of a system of
A particles requires the solution of an A body problem.
The solution of the many-body problem is itself a formidable
task, and the difficulty in solving this problem for a system
of nucleons is compounded by the lack of a quantitative
description of the nuclear force. To make any theoretical
progress in the study of nuclear systems one must take recourse
in any of several models which attempt to incorporate the
experimentally observed phenomena. All of the models have a
limited range of nuclei to which they can be applied. The
nuclear model with which we shall be concerned is the shell
model, and it is with the shell model that we will try to
understand the nuclear properties of ^{142}Praseodymium.

^{142}Pr is an unstable isotope of praseodymium in the
Lanthanide series with a half-life of 19.2(.1)hrs. The
nucleus is thought of as a system of nine protons and one
neutron outside of the doubly magic $^{132}_{50}$Sn^{132} core. Since
^{142}Pr is in the region of spherical nuclei and only ten
nucleons outside the inert ^{132}Sn core one feels justified
in attempting to describe the nucleus in terms of the shell
model. Because the nucleus is almost spherical one can
attribute the major portion of the potential that any
single nucleon feels to a central potential created by the
presence of the remaining nucleons. If the potential were
predominantly asymmetric, the nucleus would be distorted.
The non-central remainder of the force can then be treated
as a perturbation on the basic central force. In this manner

one can separate the radial and angular dependencies in the
wave function of a single particle and write for any
eigenstate

$$\psi_{nLm} = \frac{U_{Ln}(r)}{r} Y_L^m(\theta \varphi) X(s)$$

However, there exists also a spin-orbit force proportional
to $\underset{\sim}{L} \cdot \underset{\sim}{s}$ which splits the different L levels and produces the
gaps at nucleon numbers 2,8,20,28,50,82,126. The magnitude
of $\underset{\sim}{L}$ is constant since $\underset{\sim}{L}^2$ commutes with $\underset{\sim}{L} \cdot \underset{\sim}{s}$. The total
spin $\underset{\sim}{j}$ has a fixed component along the z axis. Explicitly,

$$V_{Ls} = -V(r) L \cdot s$$

so

$$\underset{\sim}{j} = \underset{\sim}{L} + \underset{\sim}{s} \qquad \underset{\sim}{j}^2 = \underset{\sim}{L}^2 + \underset{\sim}{s}^2 + 2\underset{\sim}{L} \cdot \underset{\sim}{s}$$

or

$$\underset{\sim}{L} \cdot \underset{\sim}{s} = \frac{j^2 - L^2 - s^2}{2}$$

Since this interaction is taken as a perturbation on the
central potential, to first order we can write the contribution
of the spin-orbit force to the energy of an eigenstate as

$$\langle V_{Ls} \rangle = \langle r,n,j,L,s \mid V_{Ls} \mid r,n,j,L,s \rangle$$
$$= -\langle r,n,j,L,s \mid V(r) \frac{j^2 - L^2 - s^2}{2} \mid r,n,j,L,s \rangle$$

for $\underset{\sim}{j} = \underset{\sim}{L} + \underset{\sim}{s}$
$$\langle V_{Ls} \rangle = -\left\langle \frac{V(r)}{2} _{nL} \right\rangle (L + \tfrac{1}{2})$$

for $\underset{\sim}{j} = \underset{\sim}{L} - \underset{\sim}{s}$
$$\langle V_{Ls} \rangle = +\left\langle \frac{V(r)}{2} _{nL} \right\rangle (L + \tfrac{1}{2})$$

So the L+½ level comes lower than the L-½ level, and the
spacing between levels is

$$\triangle_{Ls} = \left\langle \frac{V(r)_{nL}}{2} \right\rangle (2L + 1)$$

In figure 1 the simple shell model orbitals for protons and neutrons is presented. The diagram is from Preston(1962) p.150. , and was modified to include the observed reversal of the $3p_{3/2}$ and $1h_{9/2}$ neutron orbitals. The level ordering is the same for protons and neutrons up to $Z = 50$, and thereafter they are different. Of course,the level spacing within the proton orbitals are not the same as those within the neutron orbitals because of the coulomb potential which the protons move in.

For ^{142}Pr we shall be interested in neutron levels above neutron number 82, and proton levels above proton number 50. As was remarked earlier the neutron levels are filled to $N = 82$, and the proton levels to $Z = 50$, and these 132 nucleons are assumed to form an inert core for low excitation energies of the ^{142}Pr nucleus.

A simple shell model picture of ^{142}Pr without any other interactions would depict the nucleus as

$$\Psi(^{142}\text{Pr}) = \left(\begin{array}{cc} \underline{\qquad}\ 2d_{3/2} & \underline{\qquad}\ 3p_{3/2} \\ \underline{\quad}\text{X}\ 2d_{5/2} & \underline{\quad}\text{o}\quad 2f_{7/2} \\ \text{XXXXXXXX}\ 1g_{7/2} & \diagup\diagup\diagup\diagup\diagup\diagup\diagup\diagup\diagup \\ & 82\ \text{n} \\ \diagup\diagup\diagup\diagup\diagup\diagup\diagup\diagup\diagup\diagup & \\ 50\ \text{p} & \end{array} \right)$$
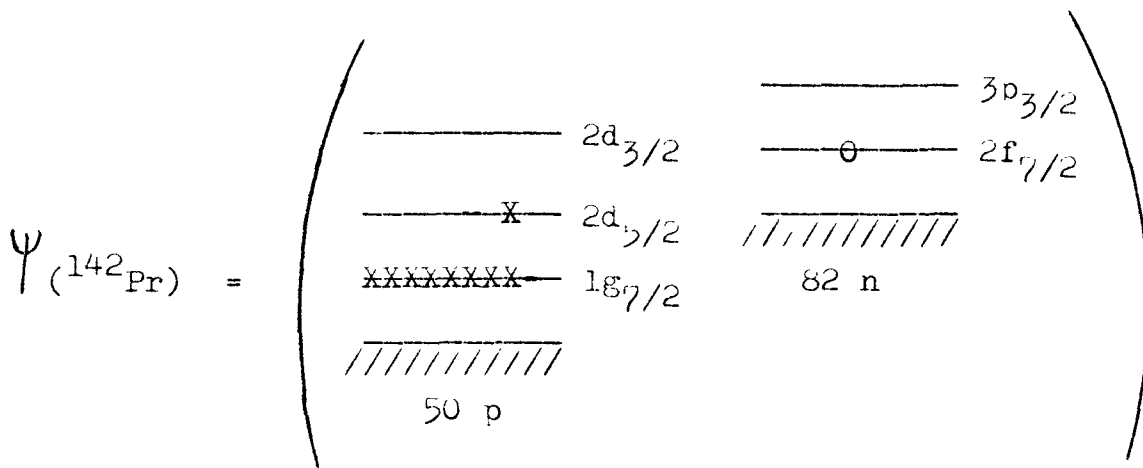
However, we know that such a simple wave function is incorrect because the protons outside the core interact with one another as well as with the odd neutron. One approach to handle the A body problem is to break up the inter nucleon

Figure 1

Neutron and Proton Orbitals In The Simple Shell Model.

Note the difference in level ordering for protons and neutrons past nucleon number 50.

126      $1i_{13/2}$

$3p_{1/2}$

$2f_{5/2}$

$1h_{9/2}$

$3p_{3/2}$

$2f_{7/2}$

82      $1h_{11/2}$

$2d_{3/2}$

$3s_{1/2}$

$1g_{7/2}$

$2d_{5/2}$

82      $1h_{11/2}$

$3s_{1/2}$

$2d_{3/2}$

$2d_{5/2}$

$1g_{7/2}$

50      $1g_{9/2}$

$2p_{1/2}$

$1f_{5/2}$

$2p_{3/2}$

50      $1g_{9/2}$

$2p_{1/2}$

$1f_{5/2}$

$2p_{3/2}$

28      $1f_{7/2}$

28      $1f_{7/2}$

20      $1d_{3/2}$

$2s_{1/2}$

$1d_{5/2}$

20      $1d_{3/2}$

$2s_{1/2}$

$1d_{5/2}$

8      $1p_{1/2}$

$1p_{3/2}$

8      $1p_{1/2}$

$1p_{3/2}$

2      $1s_{1/2}$

2      $1s_{1/2}$
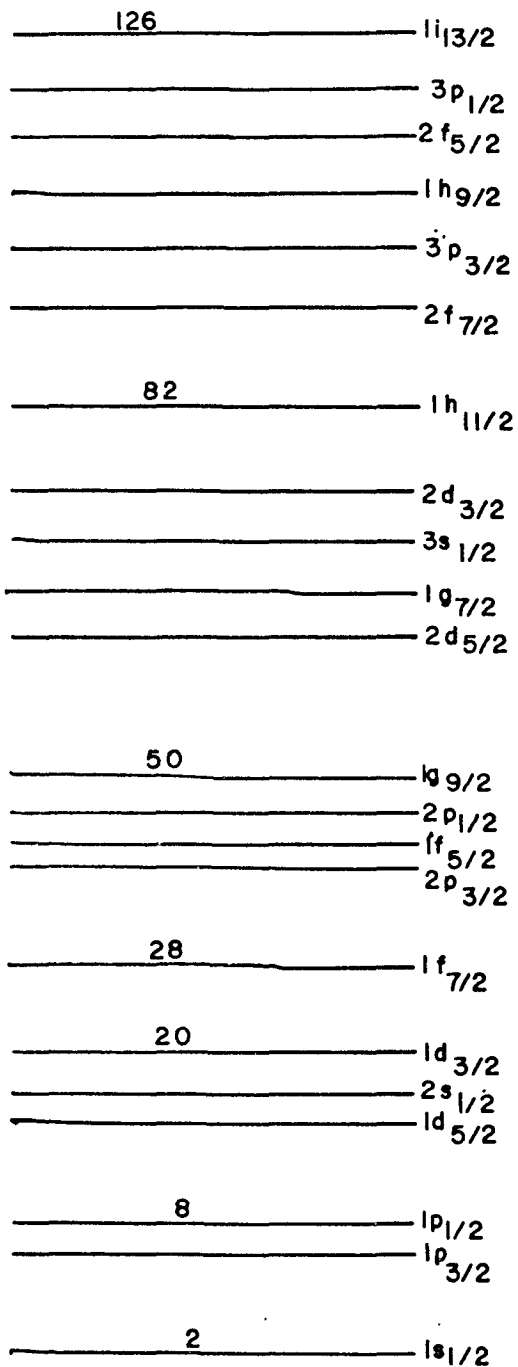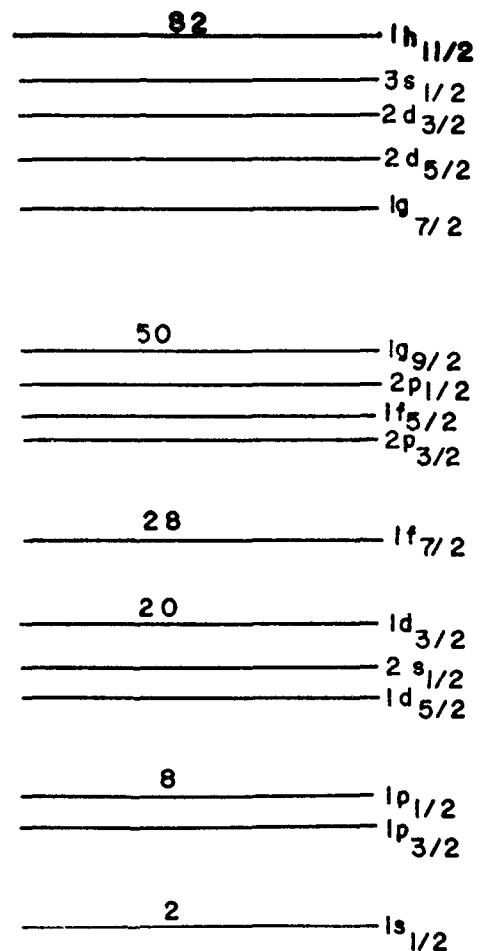
NEUTRON LEVELS   PROTON LEVELS

SIMPLE SHELL MODEL FOR THE FIRST 126
NEUTRONS AND THE FIRST 82 PROTONS

potential in a multipole expansion. That is, for A nucleons at positions $\underset{\sim}{r}_1, \underset{\sim}{r}_2, \ldots \underset{\sim}{r}_A$
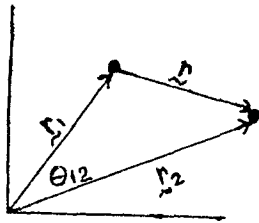
$$v(\underset{\sim}{r}_1 - \underset{\sim}{r}_2) = \sum_L v_L(r_1 r_2) P_L(\cos\theta_{12})$$

then

$$V(\underset{\sim}{r}_i) = \sum_{\substack{j=1 \\ j \neq i}}^{A} \sum_L v_L(r_i r_j) P_L(\cos\theta_{ij})$$

$$V(\underset{\sim}{r}_i) = \sum_{\substack{j=1 \\ j \neq i}}^{A} v_0(r_i r_j) + \sum_{\substack{j=1 \\ j \neq i}}^{A} v_2(r_i r_j) P_2(\cos\theta_{ij})$$

$$+ \sum_{\substack{j=1 \\ j \neq i}}^{A} \sum_{L>2} v_L(r_i r_j) P_L(\cos\theta_{ij})$$

or

$$V(\underset{\sim}{r}_i) = V_0(r_i) + \text{quadrupole term} + \text{higher L terms}.$$

For a spherical nucleus the isotropic potential $V_0(r_i)$ produces the basic (nLm) states we have been considering. The second term involving the $P_2(\cos\theta_{ij})$ represents the quadrupole forces, which can be thought of as a perturbation in the spherical nucleus, but which is a significant part of the potential in deformed nuclei. The remaining terms produce the pairing interaction. From Lane(1964),p.8 we can demonstrate that all short range effects of the potential are due to the higher multipoles.
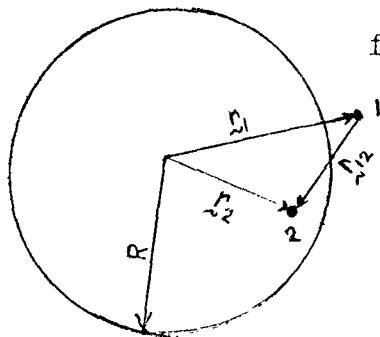
fig.1.1 from
Lane(1964)
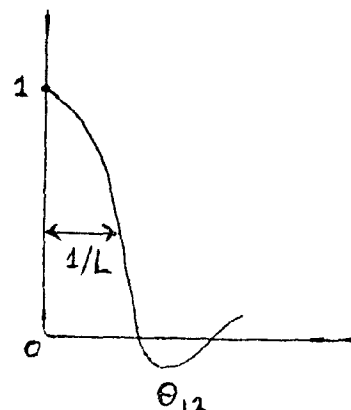
The Legendre polynomial drops from its maximum in
angular distance $\sim 1/L$. Thus the particles 1 and 2 can
interact through component L only if

$$|r_{12}| < R/L \quad , \text{ R is the mean value of}$$

$$|\underset{\sim}{r}_1| \text{ and } |\underset{\sim}{r}_2|$$

For a long range force the $L=0$ term is the most important.
But, if the force is short range the coefficients

$$v_L(r_1 r_2), \text{ if L large, must be large}$$
$$v_L(r_1 r_2), \text{ if L small, must be small}$$

Following Lane we will see what effect short range forces have
on states of $\underset{\sim}{L}^2$. We recall that for the force to be effective
the particles must lie within its range. For two particles
in orbital angular momentum states (L,m) and $(L,-m)$
the state with $\underset{\sim t}{L} = \underset{\sim}{L} + \underset{\sim}{L} = \underset{\sim}{0}$ has the form

$$U_{nL}(r_1) U_{nL}(r_2) \sum_m Y_L^m(\underset{1}{\Omega}) Y_L^{m*}(\underset{2}{\Omega})$$

But, we know that $P_L(\cos\theta_{12}) = \dfrac{4\pi}{2L+1} \sum_m Y_L^m(\underset{1}{\Omega}) Y_L^{*m}(\underset{2}{\Omega})$

and since $P_L(\cos\theta_{12})$ has its maximum at $\theta_{12} = 0$, both the
wave function of the particles and the multipole components
$v_L(r_1 r_2) P_L(\cos\theta_{12})$ have maximum values at the same place
($\theta_{12} = 0$). Thus, the states with $\underset{\sim t}{L} = \underset{\sim}{0}$ are most strongly
affected by the pairing force. Classically, $\underset{\sim t}{L} = \underset{\sim}{0}$
implies that the particles collide frequently, which just
says that they are frequently very close.
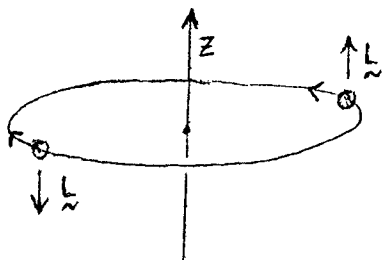
When one considers spin in addition
to orbital angular momentum, it
turns out that two particle
states of $\underset{\sim}{J} = \underset{\sim}{0}$ are most strongly

affected. Indeed, experimentally it is observed that all
even-even nuclei have ground state spins equal zero, suggesting
that the nucleon interaction in the nucleus contains
short range terms, and that these short range forces lead
to pairing.

We can note that for fermions the total wave function
must be anti-symmetric. A single particle state is
characterized by (n,j,m,t) (t = isospin). For spatially
symmetric states (L is even) $S = 0$, $T = 1$ (e.g., two protons
for which $t = -\frac{1}{2}$), the wave function need not be zero
at $r_{12} = 0$. But for spatially anti symmetric states (L is odd),
there can only be a small if not non existent effect of the
short range force on the motion of the particles since
$(r_{12}=0) = 0$.

$|\Psi|^2$
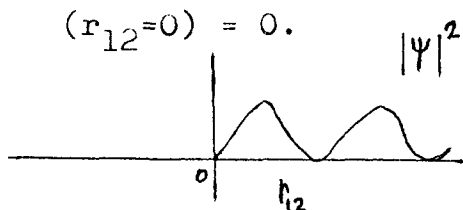
That is, the force is effective
only when the particles are
close ($r_{12} \sim 0$). But for an
anti symmetric state $\Psi(0) = 0$.

Thus, only even L states are affected by the short range
force, and of these the state $\underset{\sim}{L} = \underset{\sim}{0}$ is the most strongly
affected.

Now, if we consider a nucleus such as ^{141}Pr, we
could write the wave function as

$$\Psi(^{141}\text{Pr}) = \left(\begin{array}{l} \underline{\quad\quad\text{x}\quad\quad} \; 2d_{5/2} \\ \underline{\text{xx xx xx xx}} \; 1g_{7/2} \\ \overline{/////////////} \\ \quad 50 \; p \end{array} \quad\quad \begin{array}{l} \underline{\quad\quad\quad\quad} \; 2f_{7/2} \\ \overline{/////////////} \\ \quad 82 \; n \end{array} \right)$$
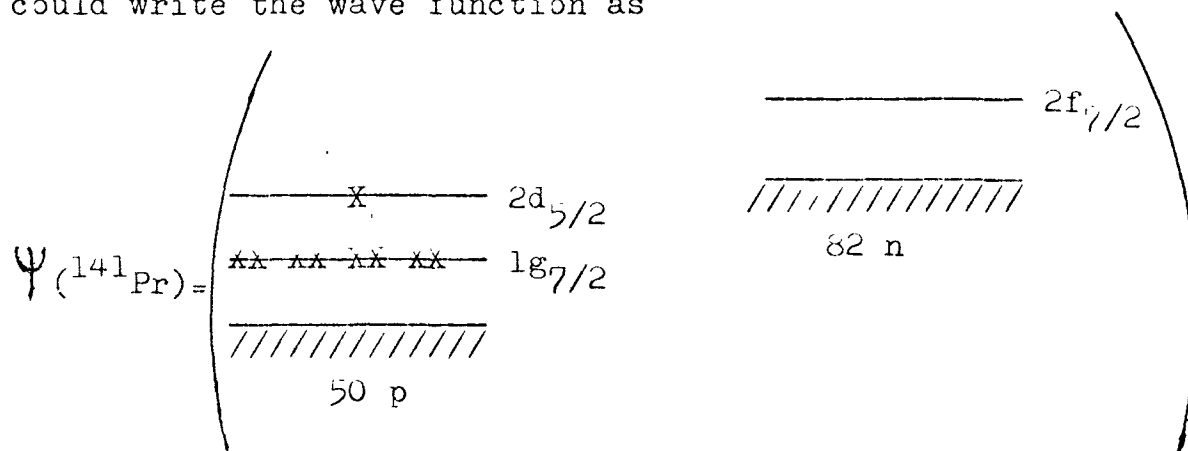
where now the protons in the $1g_{7/2}$ orbitals are paired off

to $\underset{\sim}{J} = 0$, and this leaves a lone proton in the $2d_{5/2}$ orbital.
In fact, the ground state of ^{141}Pr has spin 5/2.   Since
the nucleons are fermions, the total wave function must be
anti symmetric, and if there are A particles any state of
the system must be described by an AxA Slater determinant.
For example, for two particles 1 and 2,

$$|JM\rangle_{a.s.} = \frac{1}{\sqrt{2}} \sum_{\substack{m_a \\ m_b}} \begin{vmatrix} |j_a m_a\rangle_1 & |j_a m_a\rangle_2 \\ |j_b m_b\rangle_1 & |j_b m_b\rangle_2 \end{vmatrix} \langle j_a m_a j_b m_b | JM \rangle$$

The states (jm) could in turn be expanded in the central
field eigenfunctions. .   It is obvious that this
method can lead to quite complicated and unwieldy expressions.
If one treats the problem in second quantization the
wave functions are automatically anti symmetrized. Following
Lane (chapter 2) we can convert the hamiltonian in
coordinate space representation

$$H = \sum_i T_i + \sum_{i<j} V_{ij}$$

into occupation number representation

$$H = \sum_{\alpha,\beta} \langle \alpha | T | \beta \rangle\, a_\alpha^+ a_\beta + \sum_{\substack{\alpha\beta \\ \gamma\delta}} \langle \alpha\beta | V | \gamma\delta \rangle\, a_\alpha^+ a_\beta^+ a_\gamma a_\delta$$

where α labels the particles states and $(\alpha\beta)$ labels pair
states. The operators a_α^+ and a_α create and destroy respectively
a particle in state α. For fermions the operators must satisfy
the anti commutation rules below

$$\{a_\alpha^+, a_\beta\}_+ = \delta_{\alpha\beta} \qquad \{a_\alpha^+, a_\beta^+\}_+ = 0 \qquad \{a_\alpha, a_\beta\}_+ = 0$$

To reflect the fact that the pairing force is significant
only in states of opposite magnetic quantum number we write

$$\langle \alpha \beta | V | \gamma \delta \rangle = -|G| \, \delta_{\tilde{\alpha}\tilde{\beta}} \, \delta_{\gamma\tilde{\delta}}$$

Where $\alpha \equiv (njmL)$, $\tilde{\alpha} \equiv (nj -m\, L)$, and $|G|$ is the strength of the pairing interaction.

The aim in transforming from coordinate space to this new representation is to construct a set of non interacting quasi particles. The quasi particles are the excitations in the extra core nucleons. By breaking a pair of protons or neutrons we are creating a quasi particle. In the ground state of an even even nucleus all nucleons are paired off and thus there are no quasi particles present. Accordingly, the ground state of an even even nucleus is a quasi particle vacuum. According to Preston (1962 ,p.220) we can write the ground state of an even even nucleus with $\underset{\sim}{J} = \underset{\sim}{0}$ and seniority zero(seniority is defined as the number of unpaired nucleons) if extra core interactions are neglected as

$$\prod_\alpha |\alpha -\alpha\rangle = \prod_\alpha |\alpha\rangle |-\alpha\rangle$$

If the pairing force is included the ground state ψ_0 is

$$\alpha' \equiv nLj$$

$$\psi_0 = \prod_{\alpha'} \prod_{m>c} \left(U_\alpha |0_\alpha\rangle + V_\alpha |\alpha'm\rangle |\alpha'-m\rangle \right)$$

Where U_α^2 is the probability that the pair state (α',m) is empty and V_α^2 is the probability that the pair state (α',m) is occupied, and $|0_\alpha\rangle$ is a state for which no nucleons of type α are present. Lane(1964) shows that

$$U_\alpha^2 = \tfrac{1}{2}\left(1 + \frac{\tilde{\epsilon}_\alpha - \lambda}{\sqrt{(\epsilon_\alpha - \lambda)^2 + \Delta^2}} \right)$$

$$V_\alpha^2 = \tfrac{1}{2}\left(1 - \frac{\tilde{\epsilon}_\alpha - \lambda}{\sqrt{(\epsilon_\alpha - \lambda)^2 + \Delta^2}} \right)$$

where

$$\Delta = G \sum_\alpha V_\alpha U_\alpha \Omega_\alpha, \qquad \tilde{\epsilon}_\alpha = \epsilon_\alpha - |G|V_\alpha^2$$

and
$$N = \sum_{\alpha} 2\Omega_{\alpha} V_{\alpha}^2$$

where $\Omega_{\alpha'}$ is the number of degenerate pairs of type α' ,
i.e., if $\alpha' = nLj$ then $\Omega_{\alpha'} = j + \frac{1}{2}$.

λ is the average fermi level. If $\Delta = 0$ then $G = 0$,
and the system consists of independent particles so that
$\epsilon_{\alpha} < \lambda$, $V_{\alpha}^2 = 0$ and $U_{\alpha}^2 = 1$. $\epsilon_{\alpha'}$ is the single particle
energy in the absence of the pairing force.

The quasi particle vacuum of the even even nucleus
is then given by

$$|0\rangle = \psi_0 = \prod_{\alpha'} \prod_{m>0} \left(U_{\alpha} |0_{\alpha}\rangle + V_{\alpha} |\alpha'm\rangle |\alpha'-m\rangle \right)$$

To create a quasi particle we must break a pair. Preston
(p.222) defines the quasi particle (jm) as a mixture of
a nucleon in the state (jm) and a hole in the state (j-m).
By making the transformation from particles to quasi particles
we can study the nuclear structure via independent particles.
The quasi particles are independent of one another since
they do not act through the central field or through the
pairing force. However, they still can interact through the
quadrupole force, but for a spherical nucleus this can be
treated as a perturbation. The energy of a single quasi particle
($\alpha'm$) is given by (Lane, p 35)

$$E_{\alpha} = . \sqrt{(\tilde{\epsilon}_{\alpha} - \lambda)^2 + \Delta^2}$$

where $\tilde{\epsilon}_{\alpha} = \epsilon_{\alpha} - |G| V^2$

Since the quasi particles don't interact with one another,
the nuclear energy spectrum consists of energies

$$E_{\alpha} , \quad E_{\alpha_1} + E_{\alpha_2} , \quad E_{\alpha_1} + E_{\alpha_2} + E_{\alpha_3}, \quad \text{etc.}$$

Whereby the creation of a quasi particle (q) simply
means adding an excitation energy E_q to the nucleus.

Since the ground state of an even even nucleus
is a quasi particle vacuum, the neighboring odd nuclei
with one unpaired nucleon can be considered to be a single
quasi particle excitation of the even even nucleus. If the
unpaired nucleus is in the state (γm), the wave function
of the ground state odd nucleus is

$$\Psi_{odd} = |\gamma m\rangle \Psi_{even}$$

or

$$\Psi_{odd} = |\gamma m\rangle \prod_{\alpha'} \prod_{m>0} \left(U_\alpha | C_\alpha \rangle + V_\alpha | \alpha' m \rangle | \alpha' - m \rangle \right)$$

Thus, we can treat ^{141}Pr as a single quasi particle
excitation of the ^{140}Ce ground state with the quasi proton
in the $2d_{5/2}$ proton orbital.

Now, if we wish to study ^{142}Pr we must drop one
neutron into the ^{141}Pr nucleus. For the ground state and
low lying excitations in ^{142}Pr we expect the neutron to
occupy a state in the $2f_{7/2}$ neutron orbital. However,
the addition of the neutron introduces another interaction,
and the ground state of ^{142}Pr can not be simply the one
quasi particle excitation of the ^{140}Ce nucleus multiplied
by the neutron orbital $2f_{7/2}$. The residual neutron proton
interaction will be able to break proton pairs, thus
causing quasi particle excitations.

Using the same theoretical approach that they
employed with ^{140}La, Kern et al.(1968) claim that the
low lying states of ^{142}Pr can be described by mixing the
quasi proton $2d_{5/2}$ with the quasi proton $1g_{7/2}$. That is,
the neutron proton residual interaction mixes configurations
so that the ground state and low lying states of ^{142}Pr
should look like

That is, a quasi proton in the state $1g_{7/2}$ can couple to
the $2f_{7/2}$ neutron, and a quasi proton in the $2d_{5/2}$
orbital can couple with the $2f_{7/2}$ neutron. From these
couplings one can expect the following spins and parities
in the low lying excitations ($1g^{o}_{7/2}, 2d^{o}_{5/2}$ refer to quasi
protons in these orbitals).

$\pi 1g^{0}_{7/2}$ and $\gamma 2f_{7/2}$, $J = 0^{-}, 1^{-}, 2^{-}, 3^{-}, 4^{-}, 5^{-}, 6^{-}, 7^{-}$

$\pi 2d^{0}_{5/2}$ and $\gamma 2f_{7/2}$, $J = 1^{-}, 2^{-}, 3^{-}, 4^{-}, 5^{-}, 6^{-}$

Thus there should be fourteen states in the low lying excitations, one of spin 0^{-}, one of spin 7^{-}, and 2 each of spins 1^{-} to 6^{-}. The difference between the two 3^{-} states, say, should be reflected in different amplitudes of the $(\pi 1g^{0}_{7/2}, \gamma 2f_{7/2})$ and $(\pi 2d^{0}_{5/2}, \gamma 2f_{7/2})$ configurations. Then for a given spin JM, we have in general two states,

$$|JM\rangle_{1J} = \alpha_{1J} |\pi 2d^{0}_{5/2} \gamma 2f_{7/2}; JM\rangle + \beta_{1J} |\pi 1g^{0}_{7/2} \gamma 2f_{7/2}; JM\rangle$$

$$|JM\rangle_{2J} = \alpha_{2J} |\pi 2d^{0}_{5/2} \gamma 2f_{7/2}; JM\rangle + \beta_{2J} |\pi 1g^{0}_{7/2} \gamma 2f_{7/2}; JM\rangle$$

since

$$_{1J}\langle JM | JM \rangle_{2J} = 0 \qquad \text{we have} \qquad \left| \beta_{1J} \right| = \alpha_{2J}$$

$$\left| \beta_{2J} \right| = \alpha_{1J}$$

and Kern et al. choose the $\alpha's$ positive.
Note that for spins 0^{-} and 7^{-}

$$\left| \beta_{0} \right| = 1 \quad , \quad \alpha_{0} = 0$$
$$\left| \beta_{7} \right| = 1 \quad , \quad \alpha_{7} = 0$$

Prior to reporting on ^{142}Pr Kern et al.(1967) reported their findings on ^{140}La. They analyzed ^{140}La using the odd-odd quasi particle model we have been considering above. The theoretical detail is given by Struble(1967). Kern et al. used the (d,p) stripping reaction ^{139}La(d,p)^{140}La to locate nuclear levels in ^{140}La, and found that an independent quasi particle model adequately accounted for the relative (d,p) cross sections up to about 687 KeV excitation. At

approximately 700 kev excitation the $3p_{3/2}$ neutron orbital
makes a contribution to the possible configurations,
and at this energy the long range neutron-proton
quadrupole interaction can no longer be neglected. The
basic vector according to Kern et al(1967) at this energy
is

$$\left| j_p^0 j_n^0 \; J; pR; IM \right>$$

where

$$j_p^0 \;\; = \text{quasiproton in } \pi 1g_{7/2} \text{ or } \pi 2d_{5/2} \text{ orbital}$$

$$j_n^0 \;\; = \text{quasi neutron in } \nu 2f_{7/2} \text{ or } \nu 3p_{3/2} \text{ orbital}$$

$$p \;\; = \text{number of phonons}$$

$$R \;\; = \text{total spin of phonons}$$

$$J \;\; = \text{total spin of } j_p^0 \text{ and } j_n^0$$

$$I \;\; = \text{total nuclear spin, } I = J + R$$

Using only one phonon, i.e., pR = 12, there are 14 basis
vectors with spin 5$^-$ (spin 5$^-$ is the state in ^{140}La
at 711.7 KeV). So above 700 kev in ^{140}La the independent
quasi particle model is no longer trustworthy. On the following
page ,(Figure 2), are depicted some results from Kern
et al.(1967 and 1970) and from Struble(1967).

We will now turn our attention to ^{142}Pr exclusively
and see how successfully the above theoretical model
predicts the spins and parities of the low lying excitations
in ^{142}Pr. The ordering of the multiplets of a particular
neutron-proton configuration will be sensitive to the
neutron-proton interaction; for example,Struble(1967)
found that a delta function force could not reproduce the
experimental levels of ^{140}La. Paraphrasing Kern et al(1967);
an investigation of the level structure in odd-odd nuclei
will give information on the neutron-proton residual
interaction. We will discover that adding two protons to

Figure 2

Top: Experimental Level Structure of the Low Lying States
        in ^{140}La from the work of Kern et al.(1967) and
        Kern et al.(1970)

Bottom: Comparison of the Experimental and Theoretical
        Energy Levels in ^{140}La Using a Gaussian
        Neutron-Proton Central Interaction. Table from
        Struble(1967)

Figure 2

Experimental Low Excitations in ^{140}La
(kev)   (J-)

(kev)		(J-)
579	——————————	0
467	——————————	1
322	——————————	5
319	——————————	3
284	——————————	7
272	——————————	4
161	——————————	2
104	——————————	6
63	——————————	4
49	——————————	6
43	——————————	1
37	——————————	5
30	——————————	2
0	——————————	3

Comparison of Experimental and Theoretical ^{140}La Energy
Levels Using a Gaussian n-p Central Interaction

J-	experimental energy(Mev)	theoretical (Mev)
0	0.579	0.597
1	0.043	-0.011
1	0.467	0.404
2	0.031	0.120
2	0.162	0.102
3	0.0	0.108
3	0.319	0.395
4	0.063	0.053
4	0.272	0.241
5	0.038	0.042
5	0.322	0.513
6	0.104	-0.147
6	0.049	0.043
7	0.284	0.298

mean deviation between theory and experiment is 54 kev

^{140}La leaves the ground state and first five levels
virtually unaffected except for inverting some level orders,
and that the 7^- level in ^{142}Pr is only 70 kev above the
7^- level in ^{140}La. The implication is that the neutron
proton residual interaction is not significantly
altered between these two nuclei.

Chapter 2

Previous Research on ^{142}Pr

Overview:

The earliest work on ^{142}Pr revolved around determining the half life of the ground state decay. In the early 1950's gamma ray studies using ^{141}Pr$(n,\gamma)^{142}$Pr were reported by Kinsey et al.(1953). In the early 1960's Fulmer(1962), and Bingham(1962) reported results from (d,p) reactions in the $82 < N < 126$ region. The most extensive report on ^{142}Pr was issued in 1968 by Kern et al.(1968), and they reported finding 10 of the expected 14 low lying states formed by the $\pi 2d^{o}_{5/2})\nu 2f_{7/2}$ and $\pi 1g^{c}_{7/2})\nu 2f_{7/2}$ configurations. The four states they did not see were $0^{-}, 1^{-}, 6^{-}, 7^{-}$.

At McMaster University Hughes et al. (1966) performed ^{141}Pr(n,γ). Macphail attempted to find states in ^{142}Pr using ^{144}Nd$(d,\alpha)^{142}$Pr. His findings indicated possible states at 358 and 910 kev. Hussein using (d,p) found a level at 90(1.2)kev .

22

PREVIOUS WORK ON ^{142}PR

Ground State Decay and Half Life Measurements

All of the earliest work on ^{142}Pr was confined to measurement of the half life of the ground state decay. The earliest reported work on ^{142}Pr is the pioneering research on the production of artificial radioactivity by neutron bombardment by Fermi and co workers (1935, Amaldi et al.). These researchers found a 19 hour and a five minute activity upon bombarding praseodymium with fast neutrons. Pool and Quill(1938) demonstrated that the five minute activity was 3.5 minutes and belonged to ^{140}Pr. Marsh et al.(1935) were also active in the measurement of the half life of ^{142}Pr.

In 1942 DeWire et al. (reference B) attempted to produce ^{142}Pr by three new reactions, i.e.,

$$^{141}Pr(d,p)^{142}Pr \quad 10 \text{ Mev deuterons}$$
$$^{142}Ce(p,n)^{142}Pr \quad 5 \text{ Mev protons}$$
$$^{139}La(d,n)^{142}Pr \quad 20 \text{ Mev alphas}$$
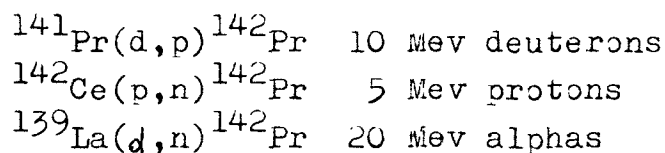
DeWire et al. found the 19 hr activity in all three of the reactions and reported a gamma ray of energy 1.9 mev for every 25 electrons in the decay.

In the late 1940's Cork et al.(1948),Mandeville(1949) Jurney(1949) and Jensen(1950) among others, measured the decay radiation of ^{142}Pr in more detail than previous workers. Jensen and co workers concluded the ground state decay scheme of ^{142}Pr as diagrammed below.
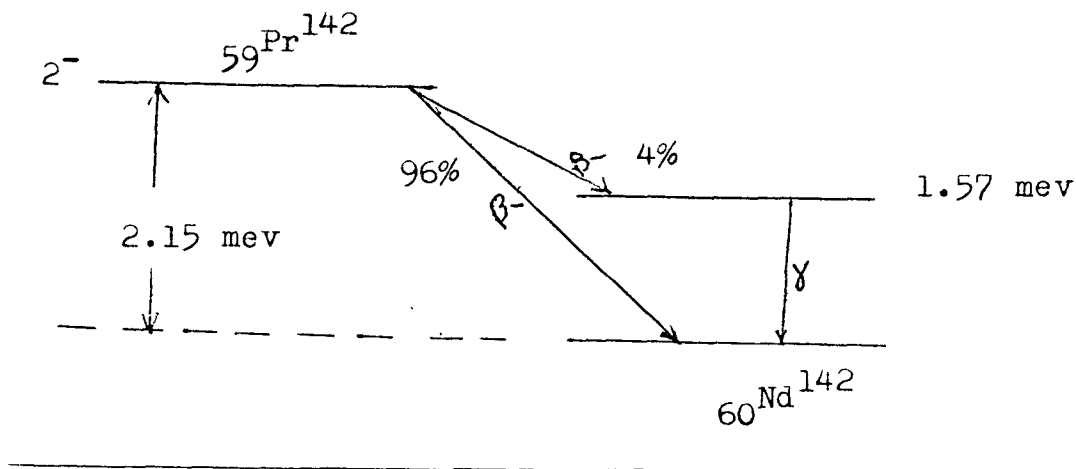
Excited States of ^{142}Pr

In 1953 Kinsey and Bartholomew measured the high energy gamma spectrum emitted by ^{142}Pr using ^{141}Pr(n,γ). The energies and intensities are listed below.

gamma energy in Mev	estimated intensity in photons/100 captured neutrons
5.83 (.03)	2
5.67 (.05)	3
5.16 (.03)	3
4.79 (.04)	2
4.69 (.04)	3

In 1962 Fulmer reported the results of stripping reactions in the 82 N 126 neutron shell using (d,p) on ^{140}Ce and ^{138}Ba. From the results of these experiments the single particle excitations in the neutron shell are as diagrammed below.

The resolution obtained in Fulmer's experiments

Mev

2.25	$3p_{1/2}$
1.9	$1h_{9/2}$
1.88	$2f_{5/2}$
0.83	$3p_{3/2}$
0.0	$2f_{7/2}$

82 neutrons

was 60 kev. The results from $^{141}Pr(d,p)^{142}Pr$ using 15 mev deuterons are given in Table II of Fulmer's paper. This table is reproduced below. The column under L refers to the neutron orbital into which the stripped neutron was transferred. For example,

$$L = 1 \text{ is a p orbital}$$
$$L = 3 \text{ is a f orbital}$$

$(d\sigma/dw)_{max}$ is the maximum differential cross section in mb/sr. Note that because of the resolution several levels are often summed together.

Table II from Fulmer(1962) $^{141}Pr(d,p)^{142}Pr$

Excitation Energy (Mev)	$(d\sigma/dw)_{max}$ (mb/sr)	L
0		
0.08	3.12	3
0.14		
0.66	1.35	1
0.78	1.54	1
0.91		
1.05		
1.14	1.82	1
1.18		
1.26	0.18	(1)
1.42	0.56	(3)
1.53	0.49	(3)
1.67	0.48	(3)
1.78	0.75	(3)
1.97	0.60	(3)
2.11	1.00	---
2.44	1.15	(1)

Also in 1962 Bingham et al. performed the same
(d,p) stripping reaction described above using 11.3 Mev
deuterons instead of 15 Mev deuterons.Their resolution
was not good enough to separate most of the levels.
Between 1.4 Mev and 2.12 Mev they saw a multitude of unresolved
states. Only one state at excitation 2.12 Mev stands out
clearly enough to be identified. Bingham et al were able to
resolve levels at 0,0.62,1.02, 1.38, and 2.12 Mev .
Below is a comparison of level schemes taken from p.1804
of Bingham et al..

2.13
1.95
1.88
1.80

1.46
1.37
1.31

1.02

0.71

0.60

0.25

^{140}La   0

2.12

1.38

1.02

0.62
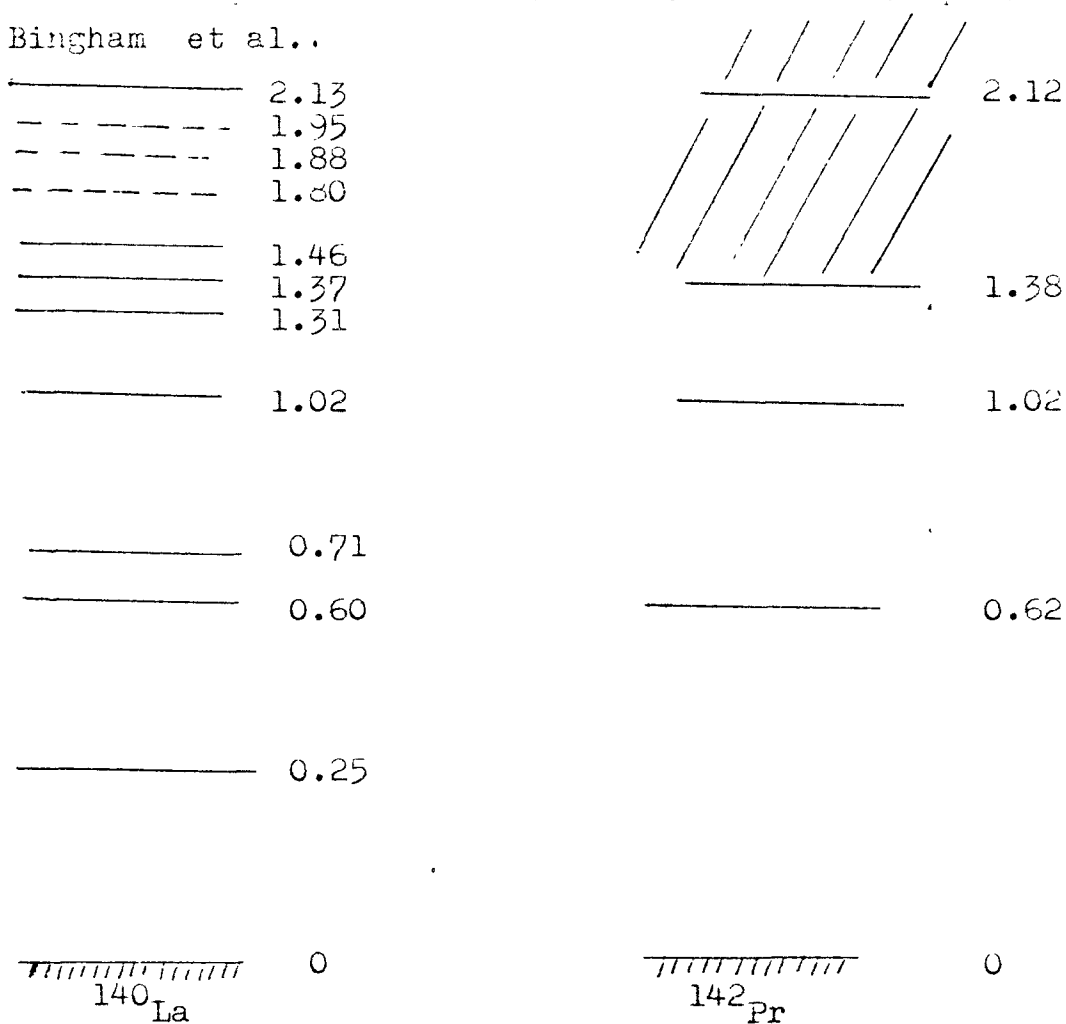
^{142}Pr   0

excitation energy in   Mev

In 1966 Hughes et al. published the results of a
thermal neutron $^{141}Pr(n,\gamma)^{142}Pr$ reaction performed at
McMaster University. Since the ground state of ^{141}Pr is
5/2+, and $L_{neutron}$=0, they expected to populate capturing
states of J = 2+ and 3+. Since the low lying states are of
negative parity, and since the ground state is 2⁻, high
energy E1 gamma transitions are expected to be prevalent.
A table of the transitions they reported is given below.

Table 4 from Hughes et al. (1966)
High Energy Transitions for $^{141}Pr(n,\gamma)^{142}Pr$

energy(± 5 kev) (kev)	relative intensity	(d,p)levels,Bingham (1962)
5842	1.52	
5823	0.53	
5767	0.36	5765 ± 30
5736	0.05	
5563	3.54	
5598	0.12	
5452	0.075	
5390	0.074	
5302	0.09	
5197	0.42	
5133	3.33	5145 ± 30
5086	1.91	
5945	0.316	
5013	0.23	
4935	0.16	
4833	0.20	
4792	1.29	
4714	0.84	4745 ± 30
4682	2.70	
4580	0.23	
4565	0.15	
4545	0.15	
4487	0.92	
4447	0.20	
4406	0.19	
4377	0.14	4385 ± 30
4360	0.425	
4337	0.25	
4314	0.19	

energy($\pm$ 5 kev) (kev)	relative intensity
4288	0.22
4267	0.33
4238	0.31
4168	0.28
4149	0.24
4117	0.24

Low Energy Transitions

energy($\pm$ 2 kev) (kev)	relative intensity
110	4.5
126	7
140	10
176	22
196	6
547	3
560	4.5
571	4
611	4.5
617	5.5
633	5
646	7
747	3.5
866	4

The most extensive report on ^{142}Pr was issued in
1968 by Kern and co workers(1968). By using a combination
of thermal neutron capture and 10 mev (d,p), Kern et al.
inferred the spins of ten of the fourteen expected negative
parity low lying states discussed in part one. By
measuring the differential cross sections of the low lying
states they were able to assign the stripped neutron to the
$2f_{7/2}$ neutron orbital. This result is gratifying in that it
is at least a partial vindication of the theoretical

coupling scheme discussed in the theory section.

A detailed argument for their spin assignments can be found in Kern et al.(1968). Basically,however, their assignments are based upon the energy combination principle(i.e.,they add energies of gamma rays to reproduce the structure observed in (d,p)) and the spectroscopic factors derived from the (d,p). They believe the $^{141}Pr(d,p)^{142}Pr$ reaction to be direct and thus the reaction cross section is proportional to the spectroscopic factor. They claim that

$$\sigma \propto \left| \left\langle \psi(^{141}Pr)n \; \middle| \; \psi^*(^{142}Pr) \right\rangle \right|^2$$

where $\psi(^{141}Pr)$ = ground state of $^{141}Pr = \left| \pi 2d^0_{5/2} \nu 2f_{7/2} \right\rangle$

n = incident neutron

$\psi^*(^{142}Pr)$ = an excited state of ^{142}Pr

Since

$$\psi(^{142}Pr)_{1J} = \alpha_{1J} \left| \pi 2d^0_{5/2} \nu 2f_{7/2} \right\rangle + \beta_{1J} \left| \pi 1g^0_{7/2} \nu 2f_{7/2} \right\rangle$$

therefore

$$\sigma_{1J} \propto (2J+1) \left| \alpha_{1J} \right|^2$$

and for state $2J$

$$\sigma_{2J} \propto (2J+1) \left| \alpha_{2J} \right|^2$$

So the (d,p) reaction enables one to select out the $\left| \pi 2d^0_{5/2} \nu 2f_{7/2} \right\rangle$ component of the wave function. Note that for $J = 0,7$, $\alpha_{1J} = 0$ and $\sigma_{J=0,7} = 0$.

By normalizing the experimental cross sections to 100 and the theoretical cross sections likewise,

$$A \sum_{i=1}^{2} \sum_{J=1}^{6} (2J+1) \, \alpha_{iJ}^2 = 100 \quad , \quad A = 2.08$$

they were able to compare average cross sections for
experimentally observed states with the theoretically
expected relative cross section. For example, the observed
levels at 17.7 and 176.9 kev have experimental relative
cross sections of 5.0 ± 0.5 and 9.9 ± 0.5 respectively.
The expected sum intensity of a pair of spin 3 levels is
14.6 (from formula above), and considering that the 176.9
kev level decays to the spin 2 ground state it is reasonable
to attach a spin 3 to the 17.7 and 176.9 kev states.
Using such a technique and the assumption that the electro-
magnetic transitions among the lower states proceed by
magnetic dipole radiation predominantly, allowed them to
build the low lying level structure on the following page
(Figure 3).

　　　　Kern and his collaborators did not observe both spin
one states and both spin six states. Consequently they
assume a very small amplitude of the $\pi 2d^3_{5/2} \nu 2f_{7/2}$ component
in the wave functions of the remaining spin 1 and spin
6 state (α = 0.10 and 0.07 respectively).
Below is a table from Kern et al.(1968) comparing the
state vectors from the (d,p) and branching ratio fits. They
maintain that their results from the gamma branching ratios
agree well with the (d,p) amplitudes for spins 3,5,6. The
agreement is acceptable for spin four, but not for spins
1 and 2.

Table IX   from Kern et al.(1968)

Level(kev)	Spin π = -	State Vector (d,p)		State Vector (gamma branching)	
		$\underline{\alpha}$	$\underline{|\beta|}$	$\underline{\alpha}$	$\underline{\beta}$
0	2	0.87	0.49	0.96	-0.28
3.7	5	0.64	0.77	0.63	-0.78
17.7	3	0.59	0.81	0.60	-0.80
63.7	6	1.00	0	0.997	0.07
72.3	4	0.34	0.94	0.22	-0.975

Figure 3

Low   Lying Nuclear States in ^{142}Pr Suggested by Kern et al. (1968).

The neutron separation energy in ^{142}Pr is 5843.4 kev
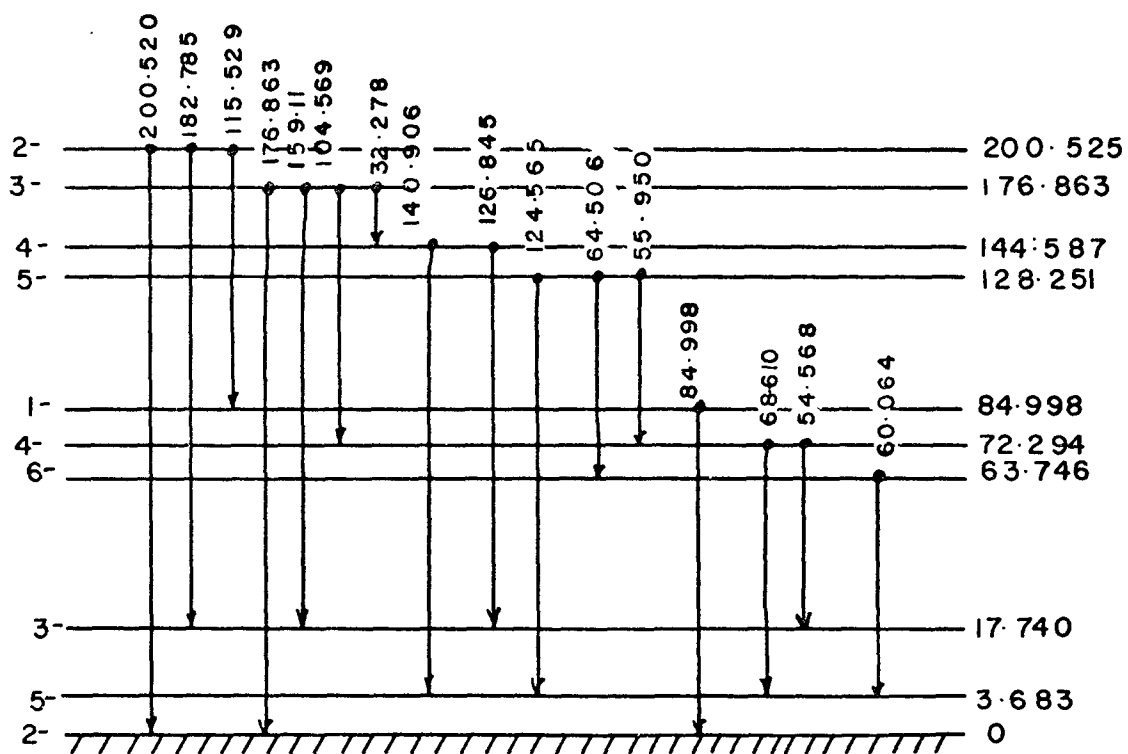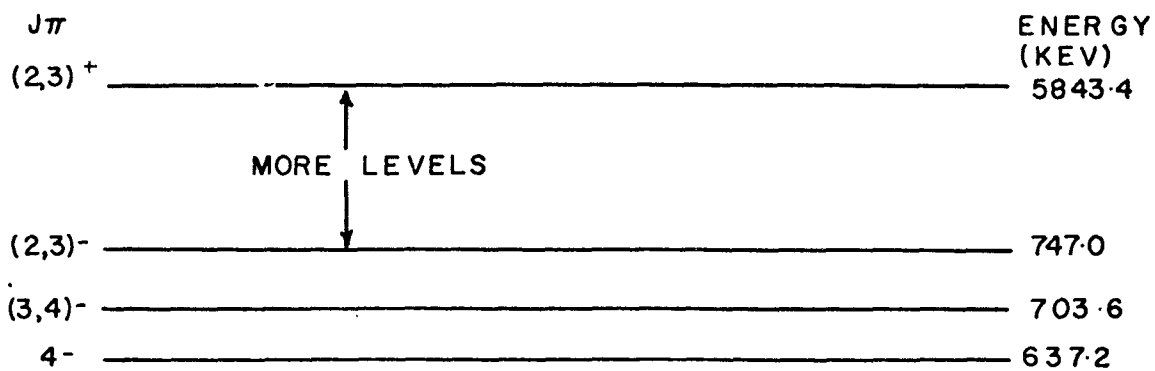
LOW LYING NUCLEAR STATES OF ^{142}PRASEODYMIUM
SUGGESTED BY KERN ETAL.

Level(kev)	Spin, $\pi = -$	State Vector (d,p)		State Vector (gamma branching)	
		α	$|\beta|$	α	β
84.9	1	0.93	0.37	0.995	0.07
128.3	5	0.77	0.64	0.78	0.63
144.6	4	0.94	0.34	0.975	0.22
176.9	3	0.81	0.59	0.80	0.60
200.5	2	0.49	0.87	0.28	0.96

These authors also attempted to extend the simple quasi particle model to levels above 200 kev. They found that the summed cross section of the low levels from 0 to 200 kev was $1429\mu b/sr$ at 45°, which agrees with the ground state cross section $1433\mu b/sr$ of ^{143}Nd (the ground state of ^{143}Nd contains a neutron in the $2f_{7/2}$ orbital). To achieve the same cross section in ^{142}Pr as the next level in ^{143}Nd (neutron in the $3p_{3/2}$ orbital) they had to add the cross sections of the next eight states from 637 kev to 1154 kev. However, on the basis of a simple model whereby the $3p_{3/2}$ neutron couples with the quasi proton in the $2d_{5/2}$ and $1g_{7/2}$ proton orbitals, only seven states are expected. That is,

$$(\pi 2d_{5/2}^0 \nu 3p_{3/2}) \quad 1^-,2^-,3^-,4^-$$

$$(\pi 1g_{7/2}^0 \nu 3p_{3/2}) \quad 2^-,3^-,4^-,5^- \quad (\text{ the } 5^- \text{ state can not be populated in (d,p) })$$

More configuration mixing may be needed to explain these states, or, perhaps we are at an energy for which coupling with the phonon vibrations of the core must be included. Recall that Kern et al.(1967) found evidence for quadrupole excitations above 500 kev in ^{140}La.

The 14.6 Minute Isomeric State In ^{142}Pr

Kern et al.(PHYS LETT, 1967) deduced the presence
of a 14.6 minute isomeric state in ^{142}Pr by following the
decay of the 1.57 Mev level in ^{142}Nd. From Kern et al.(1968)
they noted that the cross section for the formation of the
ground state in the (d,p) reaction was too large for a spin
2 state. They concluded that the peak was a doublet and noted
that their energy fits were much improved with respect to
(n,γ) if they assumed a level at 3.7 Kev . The gamma transition
from this level to the ground state is highly converted.
This level has an appreciable half life (their first
crude estimate was 7 minutes).

The spin and magnetic dipole moment of the 3.7 Kev
level has been measured by Hussein (1972) using atomic
beam resonance. Besides this spin, two other assignments
made by Kern et al were confirmed in 1970 by Mellema et al..
By ordering nuclei of ^{141}Pr in crystals of (La,Pr)$_2$Mg(NO$_3$)$_{12}$.
24H$_2$O and cooling the crystals to 0.06°K in a magnetic
field, they were able to observe anisotropies in the gamma
ray intensities as the crystal warmed up from 0.06°K to
4.2°K. They were able to make definite spin assignments of
3 and 4 to levels 17.7 and 144.6 kev respectively.

```
200  ───────────   J = 2,3,4
177  ───────────   2,3
145  ───────────   4
128  ───────────   3,4,5,6          Spin assignments
 85  ───────────   1,2,3            from Mellema et al.(1970)
 72  ───────────   3,4
 64  ───────────   3,4,5,6,7
 18  ───────────   3
3.7  ───────────
  0  ───────────
```

Recent Work At McMaster On ^{142}Pr

Besides measuring the spin and magnetic dipole moment of ^{142}Pr, Hussein (1971) undertook a series of ^{141}Pr(d,p)^{142}Pr experiments in November 1971 to try and improve on the resolution of the previous (d,p) work which we have discussed. He found among the low lying states a weak peak at 90 $\overset{+}{-}$ 1.2 kev. Now, since we can expect to observe a spin 1$^-$ or 6$^-$ among the lower levels, it is reasonable to assume that this level is the 1$^-$ or 6$^-$ level undetected by Kern et al.. If it were the 1$^-$ state, one would expect to observe a transition of 90 kev, which one does not. If it were the 6$^-$ state, one would expect to see a gamma ray of energy 90-3.7 = 86.3 kev. One does observe a gamma ray of this energy in ^{141}Pr(n,γ), ^{142}Ce(p,n), and ^{139}La(α,n). From a consideration of the systematic intensity variations of the gamma rays as a function of the initial spins from which they emanate, one concludes that the 86.3 kev transition de excites a high spin state (J > 5). This topic will be discussed at length in the next section.

Another significant measurement at McMaster was performed by Macphail (1969). He performed ^{144}Nd(d,α)^{142}Pr to search out levels not expected to be seen in (d,p). Because of a low counting rate he was able to measure the spectrum at only one angle. But his measurements did snow the peaks seen in (d,p), plus, peaks at 358 and 908 kev. In a separate experiment, ^{139}La(α,n) , he noted a strong coincidence between a gamma of energy 270(2) kev and the 85-86 kev doublet.

He believed that the $270^{\pm} 2$ kev gamma was in coincidence
with the 85 kev gamma ray and originated from the level
at 358 kev . Upon subsequent investigation it was found
that the 270 kev gamma ray was in coincidence with
the 86 kev gamma ray. This discovery is the subject of
of Chapter 4.

Chapter 3

Coincidence Technique

Overview:

>We first consider a simple circuit
>for determining the time overlap of
>two pulses. Then the general formulae
>governing the true and chance
>coincidence rates are developed.
>Next we present the schematic of the
>circuit employed in the experiments
>described in chapter 4. The function
>of each component in the circuit is
>discussed. Finally we indicate how
>the coincidence sorting program used
>in our experiments enabled us to
>separate the true coincidences from
>the chance.

The Coincidence Technique

A _____
γ_1↓
B _____ $\mathcal{T}_{1/2}$
γ_2↓
C _____

detector 1   detector 2

output of 1   output of 2

$\mathcal{T}$
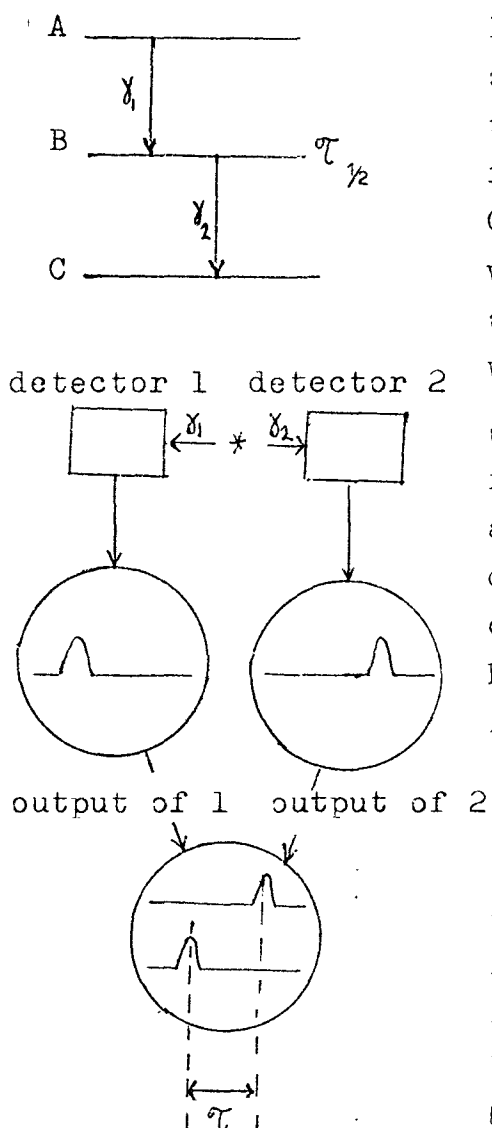
One of the more successful methods for determining nuclear level orderings is the measurement of coincident radiations. The technique can be explained by referring to the diagrams below. Consider three levels A,B,C between which gamma transitions occur. If our electronics were fast enough we could determine the half life $\mathcal{T}_{1/2}$ of state B by measuring the distribution in time between the pulses gamma 1 and gamma 2. By measuring $\mathcal{T}$ (lower diagram) we can obtain the time constant from the mean time $\overline{\mathcal{T}}$. However,typical nuclear life times for gamma emission are generally between one picosecond(10^{-12} sec) and one femtosecond (10^{-15} sec), whereas the time resolution in our experiments was of the order of 10 nanoseconds (1 nanosecond = 10^{-9} seconds). Thus, most of the time differences between gamma 1 and gamma 2 are smaller than we were capable of resolving, and consequently the pulses in our detectors are

simultaneous as far as we can measure. So, when we say
that gamma 1 and gamma 2 are in coincidence we do not mean
that levels A and B decay simultaneously, rather, gamma 1
and gamma 2 are in some form of cascade and the mean
time difference between the gammas is smaller than we are
capable of resolving.

Coincident measurements alone are not enough to tell
us the ordering of nuclear states, but in conjunction with
energy fits and gamma intensities, and other experiments,
they are a powerful method of eliminating many level schemes
which are consistent with energy fits alone.

If one uses   1cc and 50cc (active volume) Ge(Li)
detectors, one discovers that rates of 1000 counts/sec
and 20,000 counts/sec are not exceptional in a typical
experiment. The problem then becomes one of separating
true coincidence pulses from chance coincidence pulses.
First, let us consider how one is able to detect coincident
pulses, and then determine the origin of the chance coincidences.

Pulses from the detectors
have exponential shapes.
We send each pulse
through a pulse shaper
which produces a
rectangular pulse of
width τ and amplitude
V_o. If pulse 1 biases
diode 1, the diode is
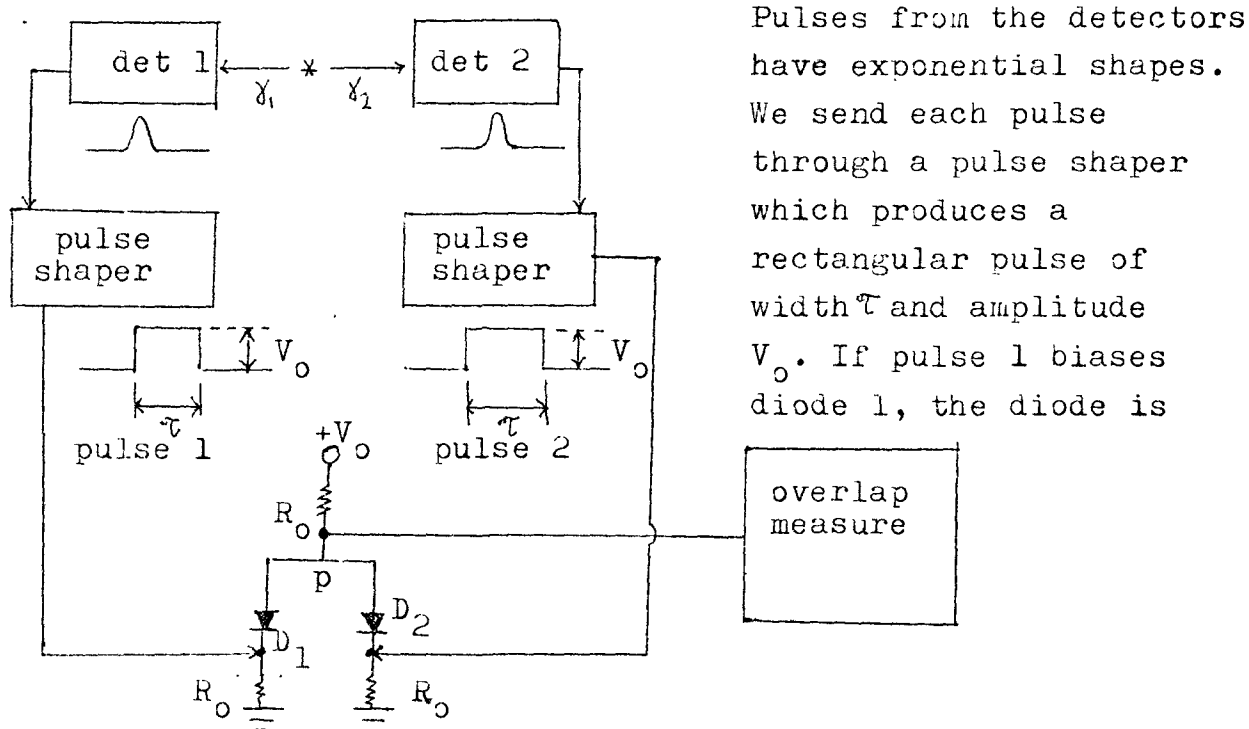
turned off and the voltage at p rises to $\frac{1}{2}V_o$. The same thing is true for a pulse incident at diode 2. If both pulses overlap for some period of time, the diodes are both turned off during the overlap period. If we set the threshold on the overlap measure above $\frac{1}{2}V_o$, we will be able to discriminate against pulses of $\frac{1}{2}V_o$, and measure only those pulses corresponding to an overlap. The circuit depicted above is not the one used in performing the experiments described in this report, but it is instructive in considering the mathematical detail which follows.

overlap of pulse 1
and pulse 2
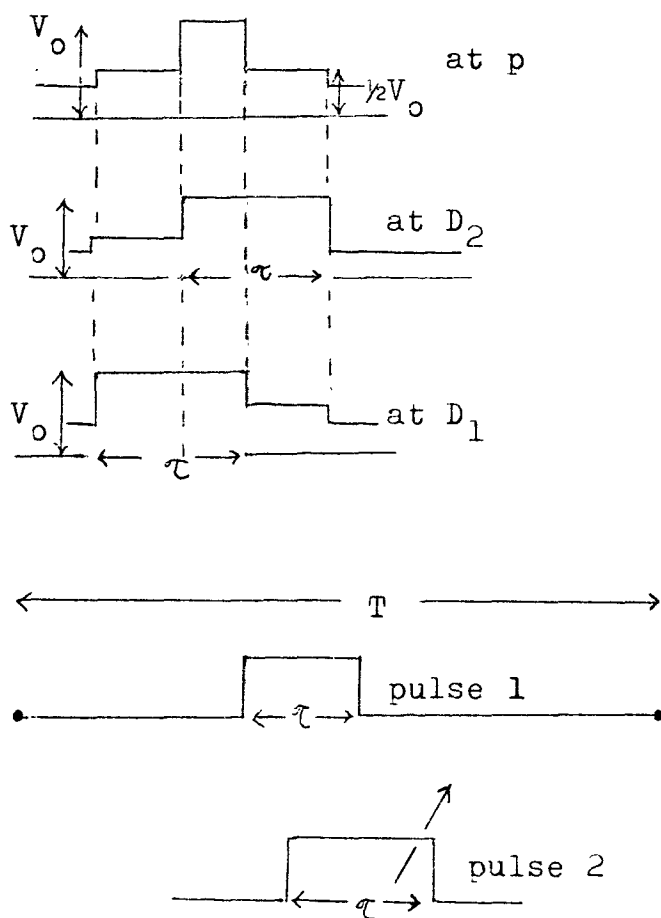
The pulse width τ is called the coincidence resolving time. We shall now consider random pulses incident on the diodes and calculate the rate of chance coincidences. The diagram below will assist us in the calculation. The simplest method of viewing a chance coincidence is by picturing it as a "scattering process". Suppose we have a total experimental time of T seconds and our pulses are of width τ. If pulse 1 occurs anywhere within time T, and pulse 2 is also equally likely at any time in T, then the probability of a

collision (i.e.,overlap) is

$$2\tau/T \ .$$

If instead of one pulse 1, there were $\overline{N}_1$ pulses in the interval T, the probability of a collision(i.e.,overlap) is

$$2\overline{N}_1\tau/T \ .$$

And, if there are also a total $\overline{N}_2$ pulses in time T as well as $\overline{N}_1$, the probability of a collision (i.e., overlap) becomes

$$2\overline{N}_1\overline{N}_2\tau/T \ .$$

If one is interested in the collison rate per second (that is, the coincidence rate), then one divides by the total time T. Thus,

$$N_c \ = \ 2\tau\overline{N}_1\overline{N}_2/T^2 \ = \ 2\tau N_1 N_2$$

where

$$N_1 = \overline{N}_1/T \quad\text{and}\quad N_2 = \overline{N}_2/T$$

where N_1 is the rate of pulses of type 1, and N_2 is the rate of pulses of type 2, and N_c is the rate of chance coincidences. If there are many types of gamma rays instead of only gamma 1, the total chance coincident rate with a particular radiation gamma i, i.e. N_c^i , will obviously be the sum over all the radiations present. Then

$$N_c^i \ = \ \sum_j \ 2\tau N_i N_j \ = \ 2\tau N_i \sum_j N_j \ = \ 2\tau N_i N_{tot}$$

where N_{tot} is the total rate at which pulses of any type are produced. Similarly the total chance coincident rate will be given by the sum of the individual totals,

$$N_c^{tot} \ = \ 2\tau N_{tot} \sum_j N_j \ = \ 2\tau N_{tot}^2 \ .$$

The N_c^{tot} above assumes that the rates of pulses at both

detectors are the same, which is not generally the case. If the total rate at detector 1 is N_{1tot} and at detector 2 is N_{2tot}, then the chance coincident rate becomes

$$N_c^{tot} = 2\mathcal{T}N_{1tot}N_{2tot} .$$

To calculate the total coincident rate we must determine the rate of true coincidences also.

$$N_{tot} = N_c^{tot} + N_t^{tot} \quad , \quad N_t^{tot} = \text{true coincidence rate}$$
$$N_{tot} = \text{total coincidence rate}$$
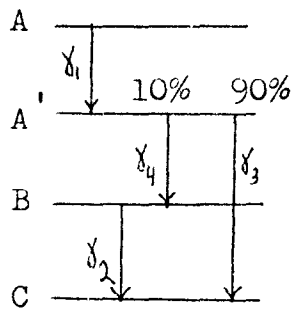
In the diagram on the left we have a more complicated level scheme than the one we were first contemplating. Suppose we wish to find the true coincidence rate between gamma 1 and gamma 2. Neglecting internal conversion, level A decays to level A' via gamma 1, and from level A' we have a ten percent chance of proceeding to level B and thus gamma 2. It is clear that there will be only one gamma 2 for every ten gamma 1's. The true coincidence rate between gamma 1 and gamma 2 is then simply 1/10 the rate of gamma 1. If we let N_t^{12} represent the true coincidence rate between gamma 1 and gamma 2,we can write

$$N_t^{12} = .1N_1,$$ and we should note that this expression is free of the coincidence resolving time $\mathcal{T}$. (Note: For the moment we will assume that we are capable of detecting all the radiation. The detectors' efficiencies and the solid angle will be included shortly.) In any experiment there are an exceedingly large number of nuclei de exciting simultaneously, so that it is

obvious that every gamma 2 that enters the detector 2 is
not in coincidence with any particular gamma 1 entering
detector 1. The total coincidence rate between gamma 1
and gamma 2 can generally be written

$$N_{tot}^{12} = 2 \tau N_1 N_2 + p_{12} N_1$$

where p_{12} is the probability that gamma 1 and gamma 2
are in coincidence. The ratio of true to chance between
gamma 1 and gamma 2 is

$$N_t^{12} / N_c^{12} = p_{12} N_1 / 2 \tau N_1 N_2 = p_{12} / 2 \tau N_2 ,$$

The true to chance ratio can be enhanced by either a small
coincidence resolving time or a small N_2 .

Thus far we have been considering an ideal situation
in which the detectors are capable of detecting all radiations
with equal probability. We have also neglected the very
significant contribution that Compton scattering makes
to the coincidence rate. Compton scattering can produce
spurious coincidences. The diagram below will help explain
this effect.
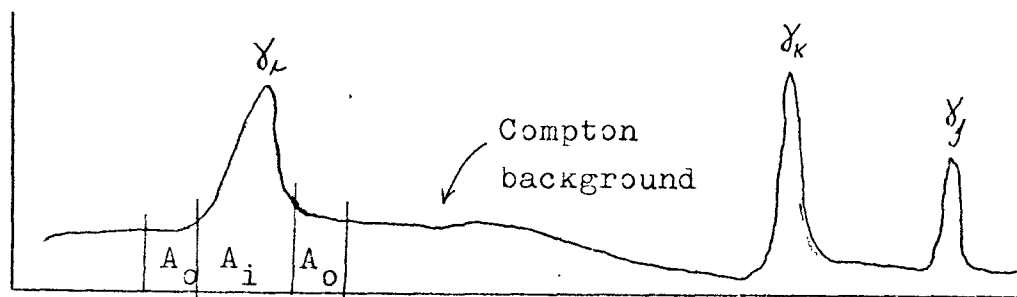
Suppose we have a gamma k whose energy is greater than
gamma i, and that this gamma k is in coincidence with a
gamma j. We know that due to Compton scattering there is
a certain probability p_{Ki}^{S} that gamma k will deposit an

amount of energy corresponding to gamma i in the detector.
We shall refer to this process by saying that " gamma k
scatters into gamma i with a probability p_{ki}^S." Thus, gamma
i appears to be produced from the scattering of gamma k,
and if gamma k is in coincidence with gamma j, then gamma i
will also appear to be in coincidence with gamma j since it
sits on the Compton background of gamma k. In fact, this
spurious coincidence rate is

$$N_{ij}^S = p_{ki}^S p_{kj} N_k$$

where N_{ij}^S is the rate at which gamma i is apparently in
true coincidence with gamma j, p_{ki}^S is the probability that
gamma k scatters into gamma i, p_{kj} is the probability that
gamma k is in coincidence with gamma j, and N_k is the rate
at which gamma k is being produced directly in the reaction.
We should note that the rate at which we detect any gamma
ray(that is, the rate at which an amount of energy equal
to the energy of the gamma ray is being deposited in our
detector) depends upon the rate at which it is being produced
in the reaction and the rate at which it is being produced
by secondary processes such as Compton scattering. We will
let

$$\tilde{N}_j = N_j + N_j^S \quad , \text{ where } \quad N_j^S = \sum_{k>j} p_{kj}^S N_k .$$

So $\tilde{N}_j$ is the rate at which gamma j appears to be produced.

Clearly the true coincidence rate can only depend
upon the direct production of gamma rays in the reaction,
and not upon the scattered gammas. Including Compton
scattering the rate of coincidence between gamma i and j is

$$N_{ij} = \underbrace{2\tau \tilde{N}_i \tilde{N}_j}_{\text{chance rate}} + \underbrace{p_{ij} N_i}_{\text{true rate}} + \underbrace{\sum_{k>i} p_{ki}^S p_{kj} N_k}_{\text{scattering rate}} .$$

If we say that gamma i goes into detector 1, and gamma j into detector 2, there is a certain efficiency of detector 1 detecting gamma i and detector 2 detecting gamma j. Let E_1^i be the efficiency of detector 1 for detecting gamma i and likewise E_2^j is the efficiency of detector 2 for detecting gamma j (effieciency includes the solid angle). Considering the efficiency of detection, the total rate at which we detect coincidences becomes

$$N_{ij} = 2\tau(N_i E_1^i + N_i^s)(N_j E_2^j + N_j^s) + p_{ij} N_i E_1^i E_2^j$$
$$+ \sum_{k > i} p_{ki}^s p_{kj} N_k E_2^j \ .$$

The chance coincidence rate and the scattering coincidence rate obscure the true rate. We have means by which we can subtract these two rates and leave only the true rate. To understand how this is accomplished we must first study the schematic circuit on the next page (Figure 4), which depicts the circuit actually used in the experiments described in this report.

List of Abreviations For the Circuit Diagram (Figure 4)

Det 1	detector 1
Det 2	detector 2
AMP	amplifier
BLR	base line restorer
D-AMP	delay amplifier
EZS	extrapolated zero strobe
TAC	time to amplitude converter
TSCA	timing single channel analyzer

Note that from each detector there are two branches. The branch proceeding through the amplifier,baseline

Figure 4

Schematic of the Coincidence Circuit Used in the
Experiments Described in this Paper.
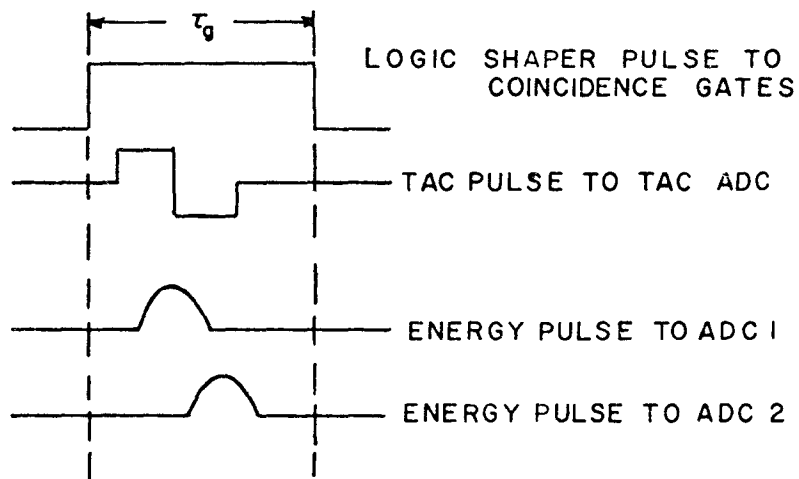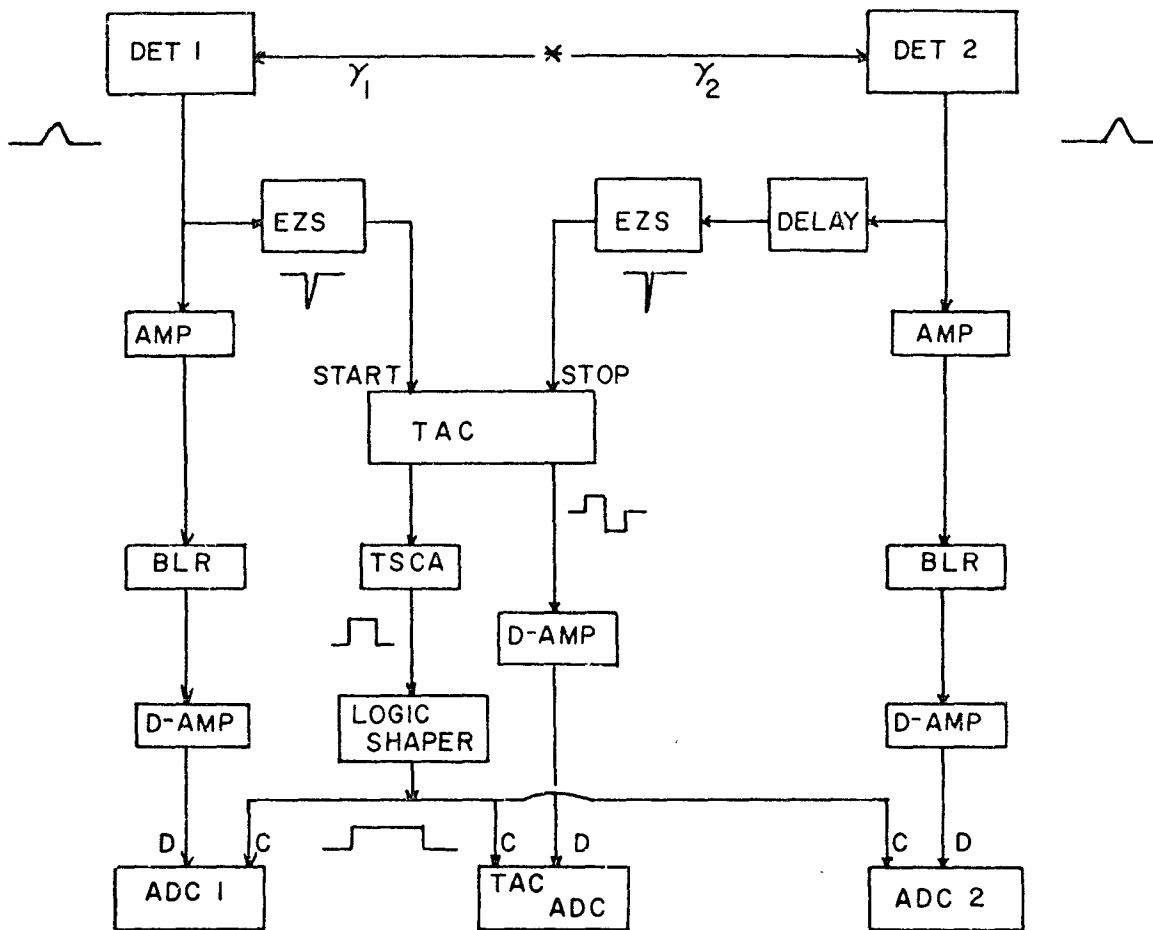
SCHEMATIC COINCIDENCE CIRCUIT

45

restorer and delay amplifier will be referred to as the "energy branch". The branch proceeding through the extrapolated zero strobe and time to amplitude converter will be referred to as the "timing branch". The central component of the timing branch is the TAC. There are two inputs on the TAC labelled "start" and "stop". The TAC can be pictured as a clock which measures the difference in time between the start pulse and the stop pulse. The clock starts when a start pulse is incident on the start input, and after receiving the stop pulse at the stop input ,it outputs a signal whose amplitude is proportional to the time difference Δt between the start and stop pulses. The TAC measures the time difference Δt by charging a capacitor during Δt, and if the capacitor C is large enough, or the difference Δt is small enough, the potential across the capacitor can be approximated by a linear function.

$$(1) \qquad (2) \qquad (3)$$
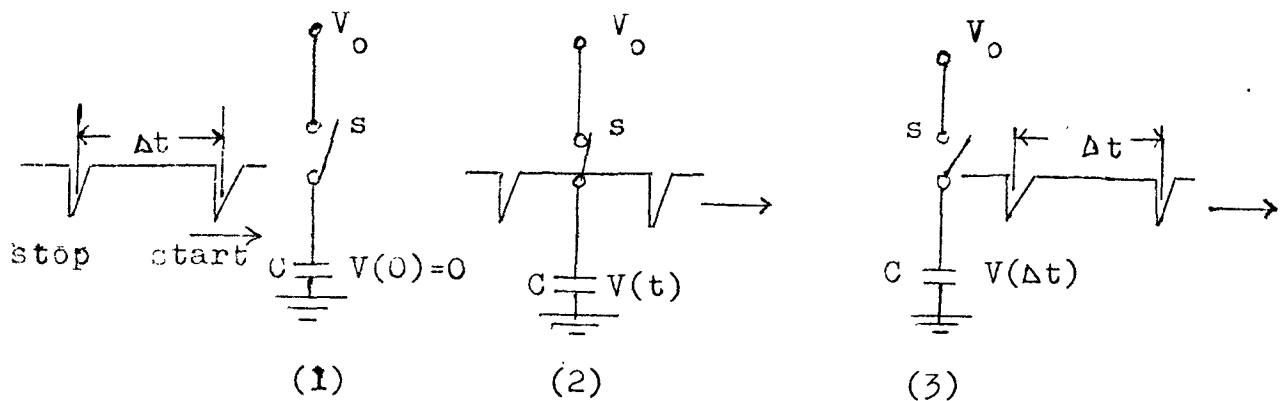
In (1) the start pulse closes the switch s, and the capacitor C charges (2) until a stop pulse opens the switch (3)· and leaves a potential $V(\Delta t)$ across the capacitor. We know that the potential across the capacitor as a function of time is

$$V(t) = V_0(1 - e^{-\mu t}) ,$$

where $\mu = 1/RC$, and R is the circuit resistance.

$$V(t) = V_0(1 - (1 - \mu t + \mu^2 t^2/2 - \mu^3 t^3/6 + \ldots))$$

and if $\mu t \ll 1$

$$V(t) = \mu V_0 t$$

The TAC that was employed in our experiments
(ORTEC Model # 437A) has an adjustable timing search, and
a maximum search period of $80 \mu sec$ ($1 \mu sec = 10^{-6}$ seconds).
By a timing search we mean the length of time the TAC will
charge before receiving a stop pulse. We can adjust the
TAC timing search such that a stop pulse must appear at the
stop input within a time Δt, $0 < \Delta t < \Delta t_{max}$, after the
start pulse. If no stop pulse is incident within this time,
the TAC automatically resets and waits for another start
pulse, without outputting a signal. In practice we set
Δt_{max} at 200 nanoseconds, so that we were only interested
in start and stop pulses less than 200 nanoseconds apart.
The TAC also has an adjustable output maximum, and the
final equation connecting the output pulse and the difference
Δt is

$$V(\Delta t) = V_0(\Delta t/ \Delta t_{max}).$$

If we set V_0 at ten volts, for example, and $\Delta t = 40$ nsec,
then

$$V(40 \text{ nsec}) = 2 \text{ volts}$$

The TAC output is sent into an ADC, and this enables
us to obtain a spectrum of Δt.

The extrapolated zero strobes fulfill two functions.
First, they shape the preamplifier pulses from the detectors
into very sharp -8 volt pulses on the order of 10 nsec
wide which are required by the TAC. Secondly they
compensate for the timing error which would otherwise be
introduced by the so called " amplitude walk ". The
amplitude walk is due to the method by which the preamplifier

pulses are produced. A gamma ray that is absorbed in the crystal (that is the Ge(Li)) produces electrons and holes proportional in number to its energy. This charge is collected on capacitor plates in the detectors, and the corresponding shape of the potential across the capacitor is again exponential. That is, for two gamma rays of energy V_1 and V_2 , neglecting constants,

$$V_1(t) = V_1(1 - e^{-\mu t})$$
$$V_2(t) = V_2(1 - e^{-\mu t})$$

and for small μt we can approximate

$$V_1(t) = V_1 \mu t$$
$$V_2(t) = V_2 \mu t$$

The preamp output can be approximated by the above two equations for small times.
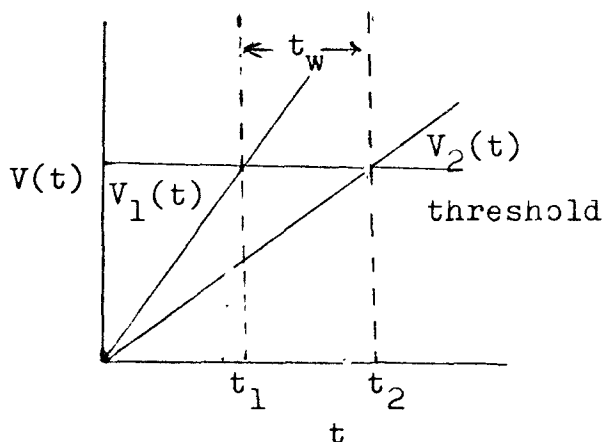
Suppose pulses of the form in the diagram are incident on the EZS input. If we had only one threshold (threshold is necessary to eliminate detector noise) and the EZS triggered whenever a pulse crossed the threshold, pulses which, in fact, were in coincidence in the detectors, are displaced by a time t_w depending upon their amplitudes. The time t_w is referred to as the amplitude walk. If there is only one threshold the pulse crosses the EZS threshold at only one point, and from this one point it is not possible to determine when the pulse originated. Consider now placing
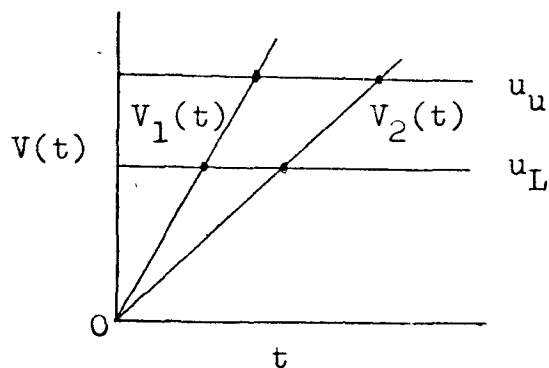
two thresholds in the
E∠S as depicted on the
left. The upper threshold
is u_u , the lower is u_L.
Since each pulse must
cross two levels to
generate an EZS pulse,
it is possible to
extrapolate back to the
zero time of each pulse
and thereby eliminate
the time walk. u_u and u_L refer to the upper and lower thresnold.

the graph shows $V(t)$ on vertical axis, t on horizontal axis, with lines $V_1(t)$ and $V_2(t)$, and horizontal lines labeled u_u and u_L

On the stop side of the timing branch we have
introduced a delay. This delay is placed in the circuit
mainly for convenience in interpreting the TAC spectrum.
To illustrate its function let us first consider a source
of completely random gamma rays. Neglecting for the moment
the scattering rate, the coincidence rate between gamma 1
and gamma 2 is given by

$$N_c^{12} = 2\tau \tilde{N}_1 \tilde{N}_2$$

Since gamma 1 and gamma 2 are completely at random, the
time interval t between them is completly random, which
means that the TAC pulse have all values of amplitude V

$$0 < V < V_0$$

equally probable. As a consequence, any particular channel
of the TAC ADC has the same likelihood of being fed as any
other channel, which means that the spectrum of Δt is a
straight line. If we now include the possibility of true
coincidences the coincidence rate is

$$N_{12} = 2\tau N_1 N_2 + p_{12} N_1$$

TAC SPECTRUM OF
RANDOM PULSES

number
of
counts

ADC channels
Δt

$^{\nwarrow}Δt_{max}$

number
of
counts

$\leftarrow\tau$

t = t_d $^{\nwarrow}Δt_{max}$
Δt
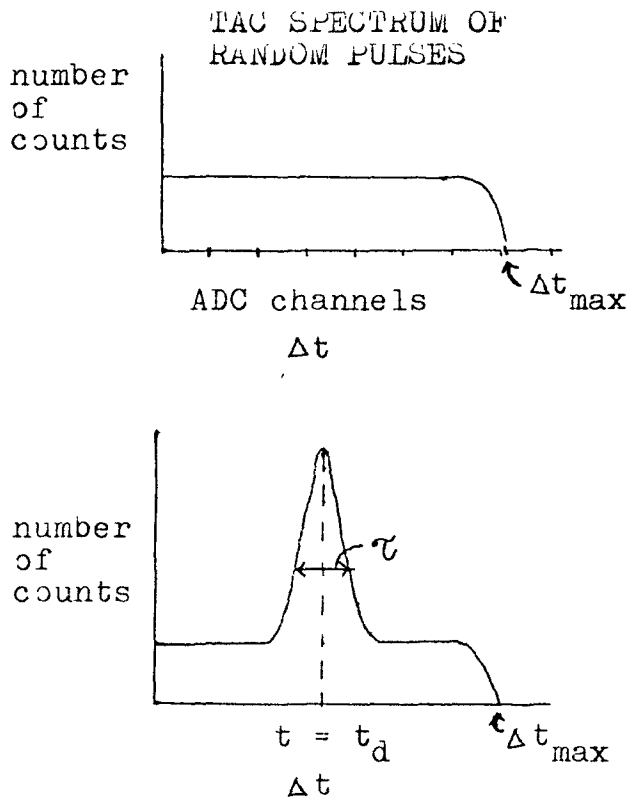
The ratio of true to chance coincidence is $p_{12}/2\,\tau N_2$ and since τ can be very small,(in our experiments τ = 10 nanosec) the Δt spectrum will have a strong peak somewhere depending upon the delay. This is depicted below. If there were no delay the peak would fall very close to or at channel zero,since $\Delta t \sim 0$. By introducing the delay t_d the coincident pulses can be delayed by time t_d , and those pulses which really are in coincidence will have a time difference at the TAC of Δt = t_d. The coincidence resolving time τ is now a function of the electronics. If the electronics were perfect and the paths between the two detectors were identical, then the peak at t_d would be a single line. But because of the variations in the delay, the cabling length,and the differences in detectors and other defects in the circuitry, the time Δt actually falls around t_d in a gaussian distribution as one would expect for a random process.

The TAC has two outputs. One is fed to the direct input of an ADC via a delay amplifier, the other goes through a timing single channel analyzer which sends out a rectangular pulse only if the input from the TAC falls between two manually adjustable levels. This pulse in turn triggers a logic shaper which also produces a rectangular pulse of adjustable width τ_g. τ_g will be referred to as the gate width, and is generally between

2μsec and 6μsec wide. The logic shaper pulse is fed to the coincidence inputs C of all three ADCs simultaneously. When the ADCs are run in the coincidence mode they will accept pulses at the direct input only while the coincidence input is activated by a pulse. The logic shaper pulse, in effect, opens the ADCs' "gates" for a period of time τ_g and allows the two energy pulses and the TAC timing pulse to enter the ADCs and be recorded. Because of the difference in circuitry that the energy pulses and the TAC pulse traverse, the three pulse will not appear in general within the gate width τ_g. To compensate for this the delay amplifiers are inserted in the circuit and adjusted so that all three pulses fall within the gate width. The delay amplifiers have gain 1 and retain the original input pulse shape. Their only function is to delay the pulses.
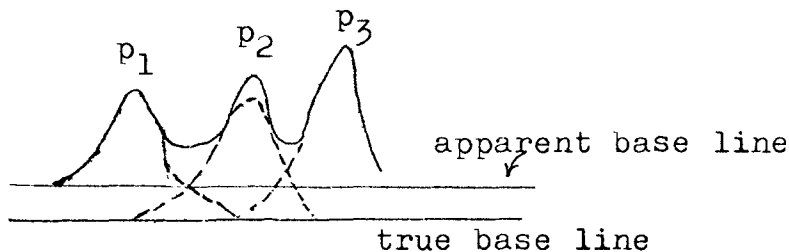
Pile Up of Pulses in an Amplifier

Finally, the base line restorers are needed if the counting rates in the detectors are too large. For a high count rate, the pulses from the amplifier may follow one another so closely that the tail of one pulse might extend under the pulse following it. As an example, p_1 and p_2 are so close in time that the tail of p_1 extends under p_2 and increases p_2's amplitude. And since the amplitude of p_2 will vary with whatever type of pulse precedes it, the corresponding peak of p_2 will be broad. Without correcting for pulse pile up the resolution for high counting rates becomes poor.

Retrieval of Coincidence Data

When the timing pulse from the logic shaper opens
the ADCs, three important pieces of information are
registered:

(1)   the energy of gamma 1

(2)   the energy of gamma 2

(3)   tne time difference Δt between gamma 1
and gamma 2

These data are, of course, recorded as channel numbers in
the appropriate ADCs. The information is stored on magnetic
tape in the form below

Δt_{ij}	gamma i	gamma j
Δt_{km}	gamma k	gamma m
Δt_{no}	gamma n	gamma o
Δt_{lp}	gamma l	gamma p
	etc	
TAC	DET 1	DET 2
ADC	ADC	ADC

magnetic tape

One can read back this tape and obtain the spectrum
contained in the DET 1 ADC column. This spectrum corresponds
to all the gamma rays that detector 1 observed that were
within a time Δt_{max} of those observed by detector 2. This
spectrum is referred to as the projection, and since we
used a one cm^3 and a fifty cm^3 Ge(Li) detector to start and
stop the TAC respectively, we have both a lcc projection
and a 50cc projection. By reading back the first column
we are able to recall the TAC spectrum, which should, as

TAC SPECTRUM

number
of
counts

(1)

T + C

C

t_w t_c

time

PROJECTION OF DET 1

number
of
counts

(2)

γ_i

γ_L

γ_m

A

A_1 A_2

energy

PROJECTION OF DET 2

number
of
counts

γ_j

γ_k

(3)

energy
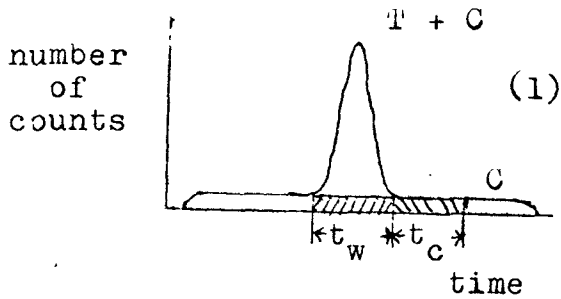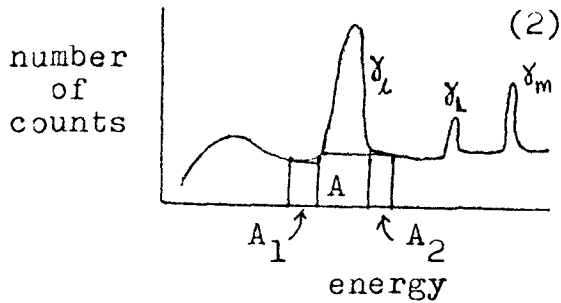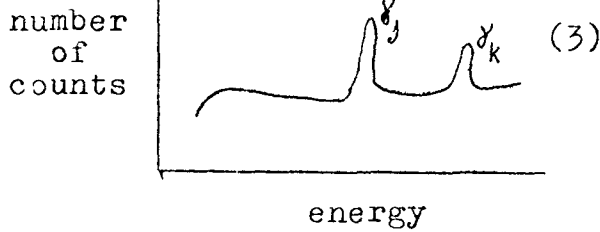
WINDOW ON γ_i IN PROJECTION OF DET 1
LOOKING INTO DET 2 PROJECTION

number
of
counts

(4)

γ_k

energy
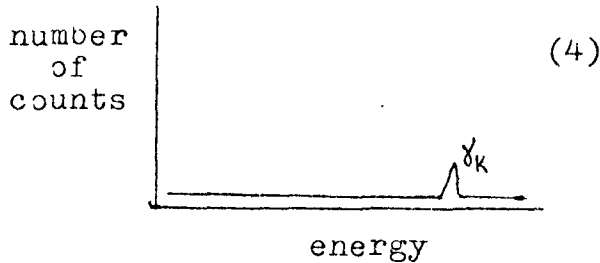
explained previously,
contain only one peak
at the delay time t_d.
With the TAC spectrum
and the two projections
we are able to sort
through the data with
the programs available
at McMaster and
determine which gamma
rays are in true
coincidence. The figures
on the left will help
explain how the sort-
ing programs operate.
The programs allow us
to set two peak windows
and three background
windows. We set the first
peak window in the TAC
spectrum on the true
plus chance (T+C)t_w
peak. To subtract the
chance coincidences
we set a window t_c in
the TAC spectrum.
Suppose we are interested
in two gammas, i and k,
in projections 1 and
2 respectively. As
the tape is read the
program comes across
combinations of gamma i

and gamma k. If Δt_{ik} is in t_c, the program subtracts 1 from
the channel number of gamma k in the spectrum of (4) on the
preceding page. If Δt_{ik} lies within t_w, the program adds 1
to the channel number of gamma k. If there are as many Δt_{ik}
in t_w as in t_c, the gammas are not in coincidence.
Along with telling the program to look for coincidences
with gamma i we must also give it information on the
background around gamma i. Since gamma i is sitting on the
sum Compton background, it is liable to be in coincidence
with anything that is in coincidence with the background.
Subtraction by the time spectrum does not remove these
spurious scattering coincidences since Δt is, in fact, t_d.
But these scattering coincidences can be removed by
finding out what is in coincidence with the immediate
background around gamma i. Since we do not expect the
Compton background to vary much (unless we are at the
Compton edge) for small energies around gamma i we
can set background windows $\Delta E_1 = \Delta E_2 = \frac{1}{2}\Delta E$. In practice
this means that the areas $A_1 = A_2 = \frac{1}{2}A$. Consequently, by
setting these background windows around gamma i, we are
able to determine how strong the spurious scattering
coincidences with gamma i are, and are thus left with
only those gammas , e.g. gamma k, which are in true
coincidence with gamma i. This is depicted in (4) on the
previous page.

Chapter 4

Experimental Work

Overview:

The major experiment performed was ^{139}La(α,n)^{142}Pr at 16.5 mev. First we consider the ^{139}La(α,n) singles experiment and present the energies and intensities of various gamma transitions. We also followed the activity of the ^{139}La target after termination of alpha bombardment.

The energies of gamma transitions in 7 mev ^{142}Ce(p,n)^{142}Pr are also presented.

Finally in the ^{139}La(α,n) 16.5 mev coincidence experiment we observed a triple coincidence between gammas of energies 86.10(.10),268.37(.10), and 552.86(.20) kev.

Set Up for ^{139}La$(\alpha,n)^{142}$Pr Coincidence
Experiment

A

1cc
Ge(Li)
detector

50cc
Ge(Li) detector

B

α beam

evacuated glass chamber

aluminum support rod
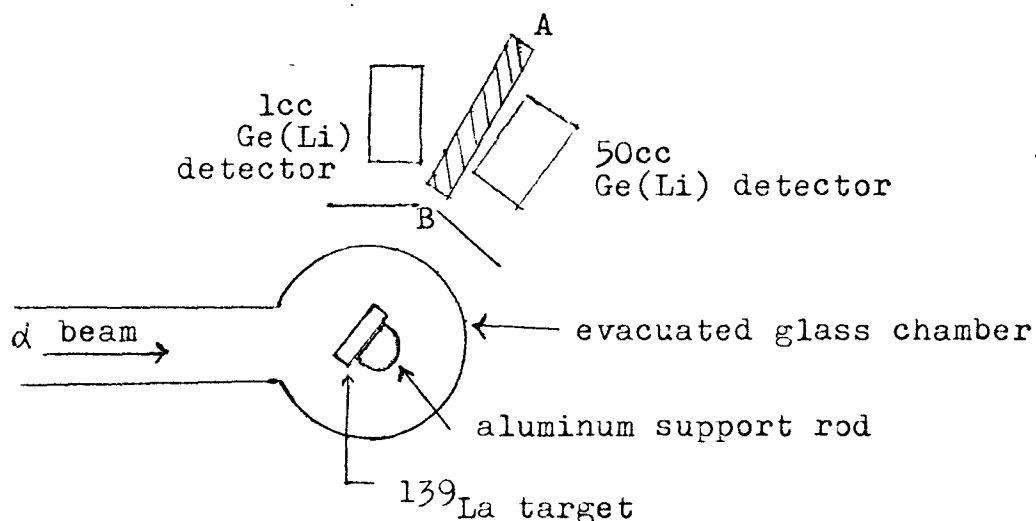
^{139}La target

The experimental arrangement which was used for
the (α,n) experiments is diagrammed above. 16.5 mev alpha
particles generated by the FN tandem accelerator impinge
upon a ^{139}La target. The target face was turned towards the
1cc detector so that low energy (less than 200 kev)
gamma rays could more easily reach the small volume detector.
Since the 50cc detector was used for energies greater than
200 kev, the thickness of the target and the aluminum
support rod provided extra shielding against low energy
gamma rays. Shielding B, in our experiments the shielding
was Mo and Cd, is used to cut down the x-ray flux from
the target. A piece of thick shielding, A, also of Mo and
Cd is used between the two detectors to prevent coincidence
measurement of Compton scattered gammas. That is, a gamma
ray incident on the 50cc detector may deposit some energy
in the 50cc detector and then scatter into the 1cc.

$$^{139}\text{La}(\alpha,n)^{142}\text{Pr} \quad \text{and} \quad ^{142}\text{Ce}(p,n)^{142}\text{Pr Singles Data}$$

Since a precise measurement of gamma ray energies is essential in unravelling the level scheme of ^{142}Pr, it is appropriate to give a brief description of the calibration and self consistency of the energies measured. The calibration sources for the 1cc and 50cc Ge(Li) detectors, along with the measure of fit χ^2, are given below.

$$\chi^2 = (1/n) \sum_{i=1}^{n} \left[(E_i^{in} - E_i^{calc})/\Delta E_i \right]^2$$

Linear Least Squares Calibration Based On Peak Centroids

1cc calibration in kev

Input	$\chi^2 = 1.2$		Output	
Source	Energy	ΔE	$E_{calculated}$	ΔE
Mo x-ray (shielding)	17.48	0.08	17.476	+.004
Cd x-ray (shielding)	23.17	0.08	23.08	+.09
$^{19}\text{F}(n,n')$	109.893	0.074	109.97	-.08
$^{139}\text{La coul ex}$	165.90	0.17	165.99	-.09
$^{19}\text{F}(n,n')$	197.147	0.084	197.32	-.17
positron annihilation	511.006	0.072	511.005	-.001

50cc calibration in kev
$\chi^2 = 1.0$

$^{19}\text{F}(n,n')$	109.893	0.164	109.61	-.28
"	197.147	0.172	197.14	-.007
positron annihilation	511.006	0.162	510.98	-.026
$^{19}\text{F}(n,n')$	1235.83	0.27	1235.55	-.28

The calibration program also makes a correction to the simple linear calibration by making a new linear calibration between calibration points that compensates for the scatter of the calculated points from the input points.

In determining the reliability of our measurements we must take into account the internal consistency of the measurements. Since we have used both 1cc and 50cc detectors in measuring gamma energies, we should expect that the energies measured be reasonably consistent from one detector to the other. In Table 1 we compare the energies of gammas detected by both 1cc and 50cc detectors from 100 kev to 600 kev. It will be noted that the standard deviation of these two sets of measurements is .40 kev. In Table 2 we compare some 50cc measurements with measurements made by Kern et al. (1968).

The measurements in Tables 1 and 2 using the Ge(Li) detectors are based on the peak centroids. Determining the energy by the centroid is not valid, however, if peaks are close enough to overlap. Consequently, a second linear calibration was made using the same sources as those used in the centroid calibration discussed on the previous page, but based on the peak positions of the source gammas. Using this second calibration the energy measured as 268.31 in the 1cc using the centroid, becomes 268.37. An examination of the (α,n) 1cc singles spectrum, Figure 5 , shows a small peak on the low energy side of the 268.37 kev gamma. Similarly, measuring the energy of the 552.55 kev gamma in the 50cc using the peak of this gamma yields 552.86.

Table 1

INTERNAL CONSISTENCY IN (α,n) BETWEEN 1cc-50cc MEASUREMENTS

(centroid calibration) *

1cc E (kev)	50cc E (kev)	$\Delta E = 1cc - 50cc$ ΔE (kev)
136.18	136.08	+.10
140.97	140.92	+.05
145.51	146.11	-.60
151.65	151.62	+.03
165.90	165.76	+.14
176.92	176.74	+.18
182.92	182.62	+.30
268.31	268.27	+.07
294.48	294.51	-.03
301.59	301.01	+.58
339.72	338.73	+.99
350.87	350.46	+.41
392.29	391.38	+.84
553.24	552.55	+.69

$\overline{\Delta} = +.24$

standard deviation = .40 kev

*Note the 50cc calibration, p.57, is consistently too low.
An apparent adjustment of +.14 kev to all the 50cc
measurements seems appropriate, but such an adjustment
is still within the uncertainty attached to the 50cc
measurements.

Table 2

COMPARISON OF 50cc MEASUREMENTS IN (α ,n) WITH KERN ET AL. (1968)

50cc (α ,n) (kev)	Kern et al.(n,γ) (kev)	$\Delta E = E(n,\gamma)-E(\alpha,n)$ (kev)
54.46	54.57	+.11
140.92	140.91	-.01
176.74	176.86	+.12
182.62	182.78	+.16
268.27	268.34(.10)	+.07
294.51 ⟵ ? ⟶ 294.81(.17)		+.30
558.56 ⟵ ? ⟶ 557.4 (.3)		-1.16
612.12	612.2 (.4)	-.08
619.3	619.9 (.7)	+.6
631.7	632.2 (.7)	+.5
645.4	645.7 (.1)	+.3
728.6	729.5 (.9)	+.9
800.2	801.1 (.7)	+.9
1107.9	1107.9(.7)	0

$$\bar{\Delta} = +.24$$

Therefore, in assessing the appropriate errors in the energy measurements we must consider the internal consistency of the measurements and the reproducibility of the calibration points. The largest deviation in the centroid calibration for the 1cc detector was -.17 kev, and this is the deviation of the raw calibration not compensating with the correction. Using the corrected calibration curve, we should expect that the calibration is not off by more than .10 kev for well formed nearly symmetric peaks in the 1cc detector. For weak peaks, or asymmetric peaks the error is larger. Similarly, for the 50cc centroid calibration the worst deviation is -.28 kev, and this magnitude of deviation occurs twice. For well formed nearly symmetric peaks in the 50cc detector one should expect an error of no more than .20 kev. For peaks which are too close together to permit us to use the centroid calibration, we use the peak position calibration . In Table 3 we have listed the gamma ray energies we observed in the 16.5 mev ^{139}La(d,n)^{142}Pr experiment. The final energies and their erros are based upon the peak shape, and the peak environment. The low energy measurements are determined by the 1cc detector, since the counting rates in the small detector are typically some twenty times smaller than the counting rate in the large detector. Also in Table 3 we have reproduced for convenience a portion of the data in Kern et al.'s paper(1968). The column under (n,γ) lists the energies they reported in ^{141}Pr(n,γ). Table 3 also contains the relative gamma intensities we observed in (d,n) correcting for detector efficiency. The intensities reported by Kern et al.(1968) are also listed.

Table 3

Comparison of Gamma Transitions Observed in ^{139}La(α,n) at 16.5 mev, and ^{141}Pr(n,γ)

E(α,n) kev	E(n,γ) kev	I(α,n) ΔI in percent	I(n,γ)
17.48[1]			
19.73[1]			
23.17[2]			
26.23[2]			
33.45[3]			
53.36*			
54.50	54.568(.008)	.80(20)	1.3(30)
60.10	60.064(.002)	28.6(23)	2.4(20)
64.63	64.506(.002)	17.2(27)	2.1(20)
67.05[4]			
68.76[4]	68.610(.002)	13.1(27)	2.0(20)
73.78[10]		15.8(32)	
78.03		12.9(17)	
84.97	84.998(.003)	3.0(-)	3.1(20)
86.10	86.056(.003)	74.0(21)	2.1(20)
93.86(.20)			
104.70	104.569(.004)	1.2(31)	.84(20)
109.89[5]			
115.59	115.529(.005)	---1---	---1---
124.69(.20)	124.565(.006)	4.4(27)	.65(20)
126.15(.20)		9.7(26)	
126.97(.20)	126.845(.003)	13.2(26)	6.2(20)
136.18[12]		1.9(29)	
140.97	140.906(.003)	17.2(26)	9.1(20)
145.51		1.8(24)	
151.65		11.6(21)	

Table 3 continued

E(α,n)	E(n,γ)	I(α,n)	I(n,γ)
159.09	159.11(.06)	1.6(21)	.31(35)
165.90[6]		7.7(21)	
176.92	176.863(.003)	22.7(19)	21(20)
182.92	182.785(.005)	9.6(18)	7.6(20)
187.78	187.79(.02)	1.1(24)	.24(40)
192.93	.	1.2(23)	
200.61(.14)	200.520(.014)	---	.76(20)
213.05(.14)		.43(16)	
225.73(.20)		1.2(24)	
230.47(.14)		.81(27)	
266.65(.28)			
268.37	268.34	53.4(12)	.50(35)
273.73(.14)		.69(34)	
294.48	294.81(.17)	11.2(16)	.69(35)
301.70(.14)[12]		1.4(27)	
339.72		6.1(17)	
350.87		21.5(13)	
373.15(.14)		1.9(28)	
379.73(.14)		2.0(30)	
392.30		5.3(23)	
404.03(.30)	403.7(.3)		
438.36(.40)[7]			
546.99(.20)	546.38(.19)		
552.86(.20)		21(25)	
557.40(.30)	557.4(.3)		
582.37(.20)			
612.12(.30)	612.2(.4)		
619.32(.30)	619.9(.7)		
631.70(.30)	631.2(.7)		
645.38(.20)	645.7(.13)		

Table 3 continued

E(α,n)	E(n,γ)
669.98(.30)	
728.62(.20)	729.5(.6)
800.18(.40)	801.1(.7)
846.80(.40)[8]	
870.77(.40)[9]	
·891.00(.20)[10]	
970.60(.40)	
1014.8(.5)	
1053.3(.5)	
1061.7(.5)	
1089.8(.5)	
1107.9(.5)	1107.9(.7)
1219.03(.5)	
1227.75(.20)	
1266.20(.30)	
1273.95(.20)[11]	

* All errors are .10 κev unless otherwise indicated
1 Mo x-ray
2 Cd x-ray
3 La x-ray
4 Au x-ray
5 ^{19}F
6 La coulomb excitation
7 ^{23}Na coulomb excitation
8 ^{56}Fe coulomb excitation
9 ^{17}O
10 ^{19}F(α,n)^{22}Na
11 ^{22}Na decay
12 ^{181}Ta

Figure 5

Gamma Ray   Spectra   Observed in 16.5mev ^{139}La(α,n)

Top: Singles Spectrum using the 1cc Ge(Li) Detector.
       Note the scale change by a factor of 10.

Bottom: Singles Spectrum using the 50cc Ge(Li) Detector.
          Gamma ray energies below 550 kev are listed
          in the 1cc singles spectrum. The scale changes
          by a factor of 3.

1cc SINGLES SPECTRUM

50cc SINGLES SPECTRUM

Activity of   La After Bombardment with 15 mev
Alpha Particles.

When our Lanthanum target was subjected to alpha
bombardment, both at 16.5 mev and 15 mev, a great deal of
gamma activity was detected after the alpha bombardment was
terminated. We detected a gamma ray of energy 1573 kev
which decayed with a half life of $20^{\pm}$ 4 hrs, and thus
assume that the gamma arises from the well established
19.2 hr decay of ^{142}Pr. The activity was followed for 8 hours.

Of the sixty five gamma transitions observed in
the decay we were able to identify only the 1573 kev, the
gammas associated with the 3.4 hr activity of ^{61}Cu, and
possibly the ground state β^{+} decay of ^{22}Na. We observed
a gamma of energy 1274.2(.7) kev in the decay, and also
in singles, and in coincidence. One would expect the 1274.6
kev transition in ^{22}Ne   to be in coincidence with
the 511 kev annihilation quanta. Moreover, in singles
we also observe gammas at 891 kev and 73 kev, and there
are similar transitions in the excited states of ^{22}Na.

Along with the above, the following energies seen
in the decay are also reported in (n, γ) by Kern et al.(1968)
and Hughes et al.(1966). The energies are in kev.

decay gamma in (α,n)	Kern et al.	Hughes et al.
907.9(.7)		907(3)
1127.8(.7)		1128(3)
1298.1(.7)		1297(3)
1726.6(.7)		1725(3)
4288.6(.7) *		4288(5)
4801.0(.7) *	4801.2(.3)	

* possible escape peaks

There was also a gamma of energy 553.5(.7) kev
seen in the decay. It seems unlikely, however, that this
is the 552.86(.20) kev gamma seen in coincidence with
the 86.10 and 268.37 kev gammas (see p. 75). Firstly,
this gamma has been measured as 553.4 kev in one experiment,
and as 553.7 kev in another, so it appears to be consistently
larger by about .7 kev than 552.86. Secondly, the gammas
with which it is in coincidence   are not seen in the
decay, and arguments considered in chapter 5 suggest that
the 553 kev transition comes above both the 86 kev and 268
kev transition.

The 553 kev gamma seen in the decay has a half life
12 $\pm$ 5 hrs.

Gamma   Rays   Observed in ^{142}Ce(p,n)^{142}Pr

The reaction ^{142}Ce(p,n) was also attempted at seven Mev. The gamma transitions observed in that reaction are listed in Table 4.

In Table 5 we have listed the common gamma ray energies between the three reactions

^{139}La(d,n)

^{142}Ce(p,n)

^{141}Pr(n,γ)
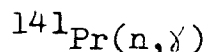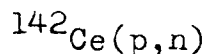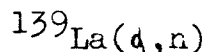
Transitions 53.36(.10)kev and 136.18(.10)kev have not been placed into the level scheme of ^{142}Pr. The two transitions

86.10(.10)kev

268.37(.10)kev

will be placed into the decay scheme of ^{142}Pr later in this thesis.

Note that the transitions (Table 5) 159.09 kev and 187.78 kev have not been seen in ^{142}Ce(p,n). The fact that this 159.09 kev transition was not noticed in the (p,n) reaction can be explained by its low intensity. In Kern et al.(1968) the ratio of the 159.11 kev intensity to the 176.86 kev intensity is

1.3/88(35%)

Or, the 159.11 kev is 67 times weaker than the 176.86 kev gamma. Since these gammas come from the same level in the scheme of Kern et al., their relative ratios should be constant. The 187.78 kev gamma has intensity 1(30%) in (n,γ) according to Kern et al.. Since this gamma originates from a spin three level in the scheme of Kern et al.(1968), and since the 176.86 kev also originates from a spin 3 state,the relative rates of increase should be the same. Consequently, in (p,n) one should expect the 187.78 kev

to be weaker than the 176.85 kev gamma by approximately
88 times, just as it is in (n,γ). The weakest intensity
gamma that we do observe in (d,n),(p,n) and (n,γ) is the
124.56 kev gamma, which is twice as intense as the 159.11
kev gamma in (n,γ).

Table 4

Gamma Transitions Observed in ^{142}Ce(p,n) With
7 MEV Protons

E (kev)	Δ E (kev)
53.48	.20
54.34	.30
59.99	.10
64.63	.15
85.02	.15
86.10	.15
104.55	.15
115.55	.15
124.53	.15
126.85	.15
129.73	.15
132.82	.40
136.14	.15
140.92	.15
143.31	.15
147.10	.15
160.67	.30
163.90	.40
169.31	.15
176.89	.15
182.81	.15
190.59	.15
200.74	.15
219.02	.15
243.40	.15
338.0	.4
363.7	.4
383.0	.4
403.0	1.0

Table 5

Common Gamma Energies in ^{139}La(α,n), ^{142}Ce(p,n), ^{141}Pr(n,γ)
Using 16.5 mev Alpha Particles, 7 mev Protons.*

^{139}La(α,n)16.5mev $E\gamma$ (kev)	^{142}Ce(p,n)7 mev $E\gamma$ (kev)	^{141}Pr(n,γ) $E\gamma$ (kev)
53.36(.10)	53.48(.15)	
54.50(.10)	54.34(.30)	54.568(.008)
60.10(.10)	59.99(.15)	60.064(.002)
64.63(.10)	64.63(.15)	64.606(.002)
84.97(.10)	85.02(.15)	84.998(.003)
86.10(.10)	86.10(.15)	86.056(.003)
104.70(.10)	104.55(.15)	104.569(.004)
115.59(.10)	115.55(.15)	115.529(.005)
124.69(.10)	124.53(.15)	124.565(.006)
126.97(.10)	126.85(.15)	126.845(.003)
136.18(.10)	136.14(.15)	
140.97(.10)	140.92(.15)	140.906(.003)
159.09(.10)		159.11(.06)
176.92(.10)	176.89(.15)	176.863(.003)
182.92(.10)	182.81(.15)	182.785(.005)
187.78(.10)		187.79(.02)
200.61(.10)	200.74(.15)	200.520(.014)
268.37(.10)		268.34(.10)
404.0 (.3)	403.0(1.0)	403.7(.3)

* All of these gammas have been placed into the ^{142}Pr
level scheme, except for 53.36,136.18,86.10,and
268.37. The 86.10 and 268.37 kev transitions will
be placed in the level scheme later in this paper.

Figure 6

Top: Singles Spectrum Collected with the 1cc Ge(Li)
         Detector in 7 mev ^{142}Ce(p,n). The scale changes by
         a Factor of 4.

Bottom: Coincident Gammas Seen by the 50cc Ge(Li)
         Detector with a Window on the 85-86 kev
         Doublet in the 1cc Projections.
         Note the low energy cut off in the spectrum is
         115 kev.

$^{142}Ce(p,n)^{142}Pr$ SINGLES SPECTRUM

7 Mev PROTONS
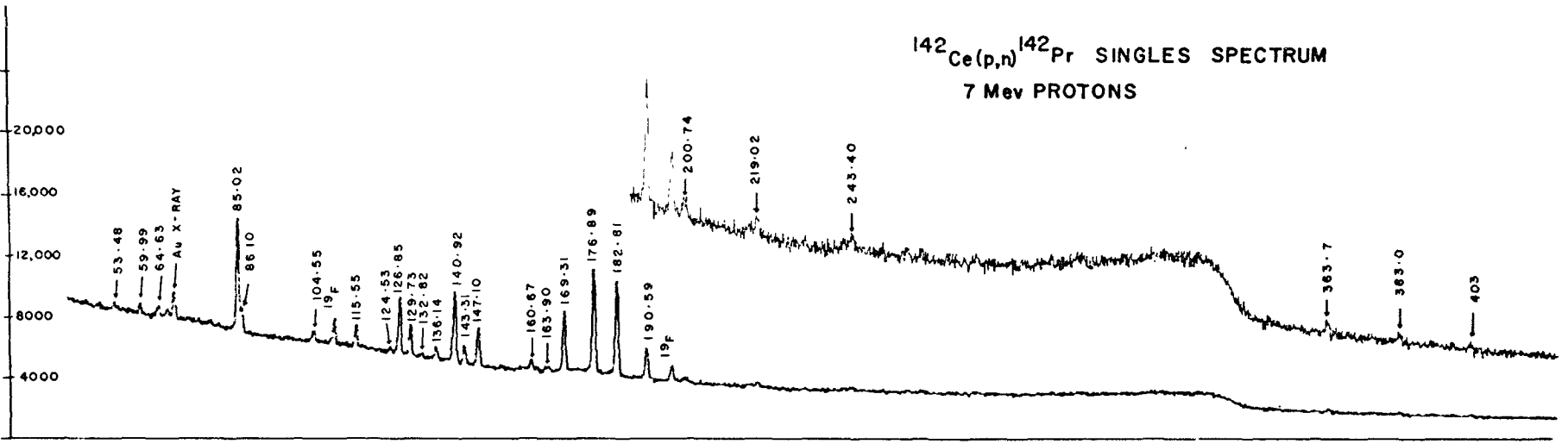
85 & 86 kev WINDOW IN 1 cc
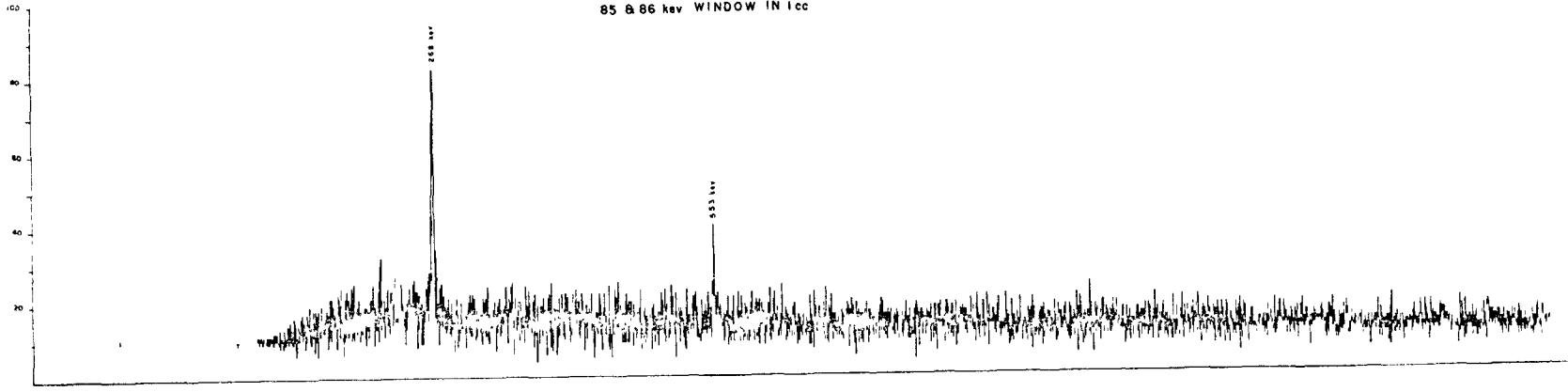
Top: Figure 7

Coincident gammas seen by the 50cc Ge(Li) detector
with a window on the 268 kev gamma in the 1cc
projection.

Bottom: Figure 8

Coincident gammas seen by the 1cc Ge(Li)
detector with a window on the 268 kev gamma
in the 50cc projection.

268 KEV WINDOW IN 1cc

268 kev WINDOW IN 50cc
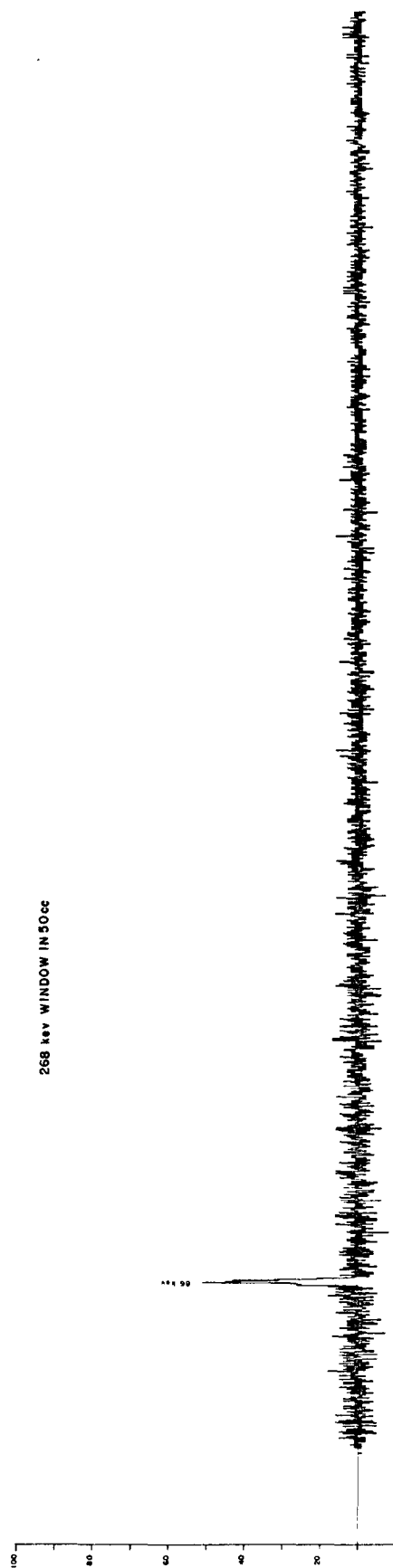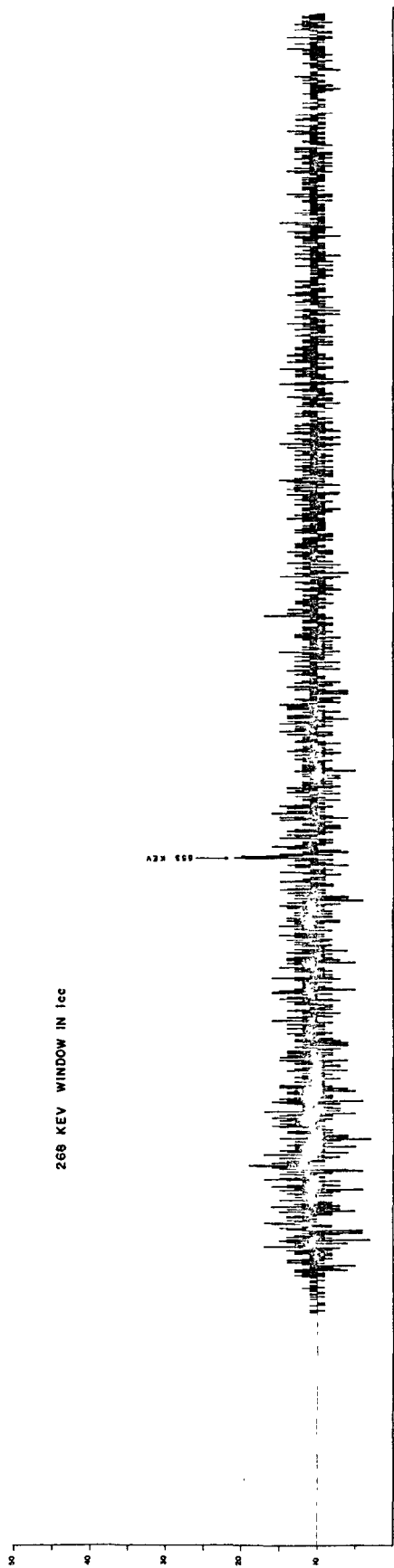
Figure 9

Coincident gammas seen by the 1cc Ge(Li) detector
with a window on the 552.86 kev gamma ray in the
50cc projection.

Figure 10

Time spectrum obtained for the coincidence
experiment described in this paper. The
coincidence resolving time was 10 nanoseconds.

TAC SPECTRUM

10 nanoseconds
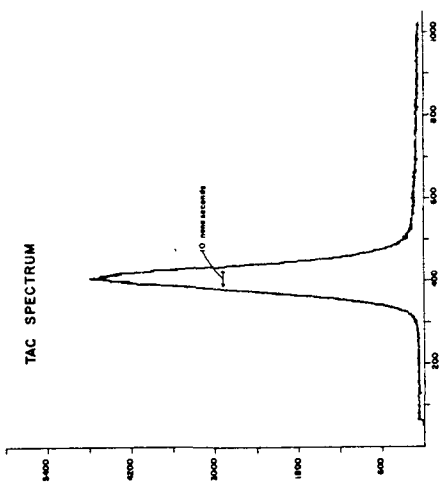
553 kev WINDOW IN 50 cc

268 kev

88 kev
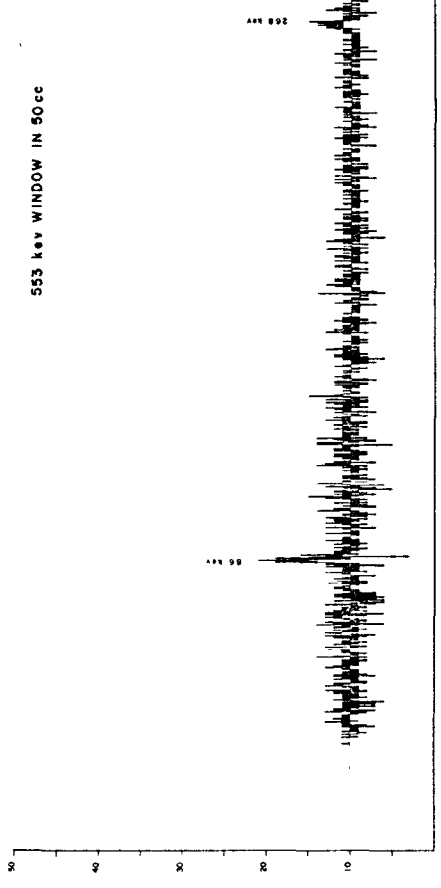
Figure 11

Top: Projection spectrum collected by the 1cc Ge(Li)
        detector during the   16.5 mev ^{139}La(α,n)
        coincidence experiment. The projection includes
        gamma rays between 20 kev and 600 kev.

Bottom: Projection spectrum collected by the 50cc Ge(Li)
        detector during the 16.5 mev ^{139}La(α,n)
        coincidences experiment. The projection includes
        gamma rays between 115 kev and 1300 kev.

Icc PROJECTION

50 cc PROJECTION

The ^{139}La(d,n) Coincidence Experiment

At 16.5 mev the reaction ^{139}La(d,n) produces,
among others, two gamma rays of energies

$$84.97(.10) \text{ kev}$$
$$86.10(.10) \text{ kev}$$

These gammas have the intensity ratio in singles

$$I_{85}/I_{86} = 1/25$$

Coincidences are observed between this doublet
and gammas of energy 268.37(.10) and 552.86(.20) kev.
Figure 6 displays the spectrum obtained looking through
the 85-86 kev doublet into the 50cc detector. Figure 7
is what is seen looking through the 268 kev window in the
1cc detector. Figure 8 is obtained by setting windows in
the 50cc detector on the 268 kev gamma and looking into the
1cc detector. Figure 9 is the spectrum of coincident
gammas looking through the 553 kev window in the 50cc.
From the spectra in Figures 8 and 9 and from a comparison
of the 1cc singles spectrum(Figure 5) and the 1cc
projection spectrum(Figure 11),one is able to conclude that
the coincident gamma in the 85-86 doublet is the 86 kev
transition , and that it is uncertain that the 85 kev gamma
is also in coincidence with the 268. This is so because of
the poor resolution in the projection spectrum (Figure 11).
Consequently, within our measurements, the 268.37 and
552.86 kev gamma are certainly in coincidence with the
86 kev gamma.

Chapter 5

Discussion

Overview: .

Using the results of the coincidence
experiment, and the results of
Hussein's ^{141}Pr(d,p) experiment
we attempt to justify placing
three new nuclear levels in
^{142}Pr at 89.739(.006) kev,
358.11(.10) kev, and 910.97(.30)
kev . We consider the implications
of the intensity variations of the
gamma transitions from these
three levels to determine possible
spin assignments. We also find
that a gamma of energy 294.48(.10)
kev seen in ^{139}La(α,n) can be
explained as a transition from
the suggested level at 358 kev to
the level at 63.7 kev. The branching
ratio of the 294.48 kev gamma in
^{139}La(α,n) yields the same component
of the $\pi 2d_{5/2}^{c} \nu 2f_{7/2}$ in the level
at 90 kev as does Hussein's (d,p) work.

DISCUSSION

The simplest ordering of the three coincident
gamma rays, 86.10,268.37, and 552.86 kev, is a direct
cascade. If this is assumed it remains to determine the
location of this cascade in the nucleus. A pivotal experiment
in placing these transitions was performed by Hussein.
Using 10 mev protons in ^{141}Pr(d,p) he reported a weak
level of intensity 1.8(.8) (relative intensity out of
100) existing at 90 $\pm$ 1.2 kev. Kern et el. did not find the
levels of spins $0^-,7^-,1^-,6^-$. Since we do not expect the
spins 0^- and 7^- states to be populated in (d,p), this new
level presumably is the spin 1^- or 6^- state. If this
90 kev level were the missing 1^- state we should expect it
to preferentially decay to the 2^- ground state. Now, a gamma
of energy 93.86(.10) is seen in ^{139}La(α,n) at 16.5 mev, but
it is not seen in ^{141}Pr(n,γ), or in ^{142}Ce(p,n) at 7 mev
proton energy. In view of the fact that the capturing state
in (n,γ) is 2^+ or 3^+ , we should expect that high energy
E1 transitions would populate this hypothesized 1^- state
fairly strongly. Moreover, a gamma of energy 93.0 kev is
seen in the target activity after (α,n). In view of the
foregoing facts, it appears unlikely that the level at
90 kev observed by Hussein is the 1^- state. Thus, we are
left with a possible spin assignment of 6^-. If this state
did have spin 6^-, we could expect it to preferentially
decay to the 5^- isomeric state at 3.7 kev. Indeed, if one
adds the energy of the 86.10(.10) kev gamma to the energy
of the 3.683 kev isomeric state, one obtains an energy
89.78 kev. Thus, we could account for the 86.10 kev gamma

as a transition between the state at 89.78(.10) kev and the
3.7 kev isomeric state.

If we then place the 268.37 kev transition directly
above the 86.10 transition we obtain a level at 358.11(.10)
kev (using Kern et al.s' more precise value 86.056(.003)
kev). Since this level decays to the suggested 6⁻ level
at 89.739(.006) kev , one could also expect the possibility
of another transition to the remaining 6⁻ level at 63.746
kev. In fact, this transition from 358.11(.10) to 63.75 kev
should be 294.36(.10) kev, and we see a gamma in (d,n)
at 294.48(.10) kev. Continuing in our assumption of a direct
cascade, the 552.86(.20) kev gamma when added to the
hypothetical state at 358 kev yields a state at 910.97(.30)
kev. The suggested decay scheme for the three coincident
gammas can be seen in Figure 13. In any event, it appears
improbable that the 553 kev gamma is the bottom member of
the triad because

    (a) no 553 kev gamma is reported in (n,γ)
        by Kern et al.(1968)

    (b) no 553 kev transition is observed using
        15 mev alpha particles in ^{139}La(d,n),
        despite the presence of the 268 and 86
        kev gammas.

A study of relative gamma intensities as they change
from one reaction to another can also yield information
on the spins of nuclear states. If we compare the relative
gamma intensities in ^{141}Pr(n,γ) with those in ^{139}La(d,n),
a significant increase in relative gamma intensities
is noted if plotted as a function of the spin of the initial
state from which the gamma ray emanates. Higher spins
should be preferentially populated in (d,n) than in (n,γ).
This is reasonable because the spin of ^{141}Pr ground state

Table 6

Dependency of $I_\gamma(q,n)/I_\gamma(n,\gamma)$ on the Spin
of the Decaying State

DEPENDENCY OF RELATIVE GAMMA INTENSITIES FROM ^{139}La(α,n) TO ^{141}Pr(n,γ) ON THE SPIN OF THE DECAYING STATE

INITIAL SPIN	E kev	$I_\gamma(\alpha,n) / I_\gamma(n,\gamma)$
1	84·97	3·1/3·0 = 1
2	182·92	9·6/7·6 = 1·3(38%)
3	104·70	1·2/·84 = 1·4(51%)
	176·92	22·7/21= 1·1(39%)
	159·09	1·6/·31 = 5·1(56%)
4	68·76 [1]	
	54·50	·80/1·3 = ·6(50%)
	126·97	13·2/6·2 = 2·1(46%)
	140·97	17·2/9·1 = 1·9(46%)
5	64·63	17·2/2·1= 8·2(47%)
	124·69	4·4/·65= 6·8(47%)
6	60·10	28·6/2·4= 11·9(43%)

[1] gold x rays from the detector obscure this ratio

Figure 12

Variation of Gamma Ray Intensities as a Function of the
Spin of the Decaying State.

$$\frac{I_\gamma(\alpha,n)}{I_\gamma(n,\gamma)} = \delta \quad vs \qquad SPIN \ OF \ DECAYING \ STATE$$

HEAVY LINES ARE SUGGESTED INITIAL SPINS OF
86·10 AND 268·37 kev TRANSITIONS
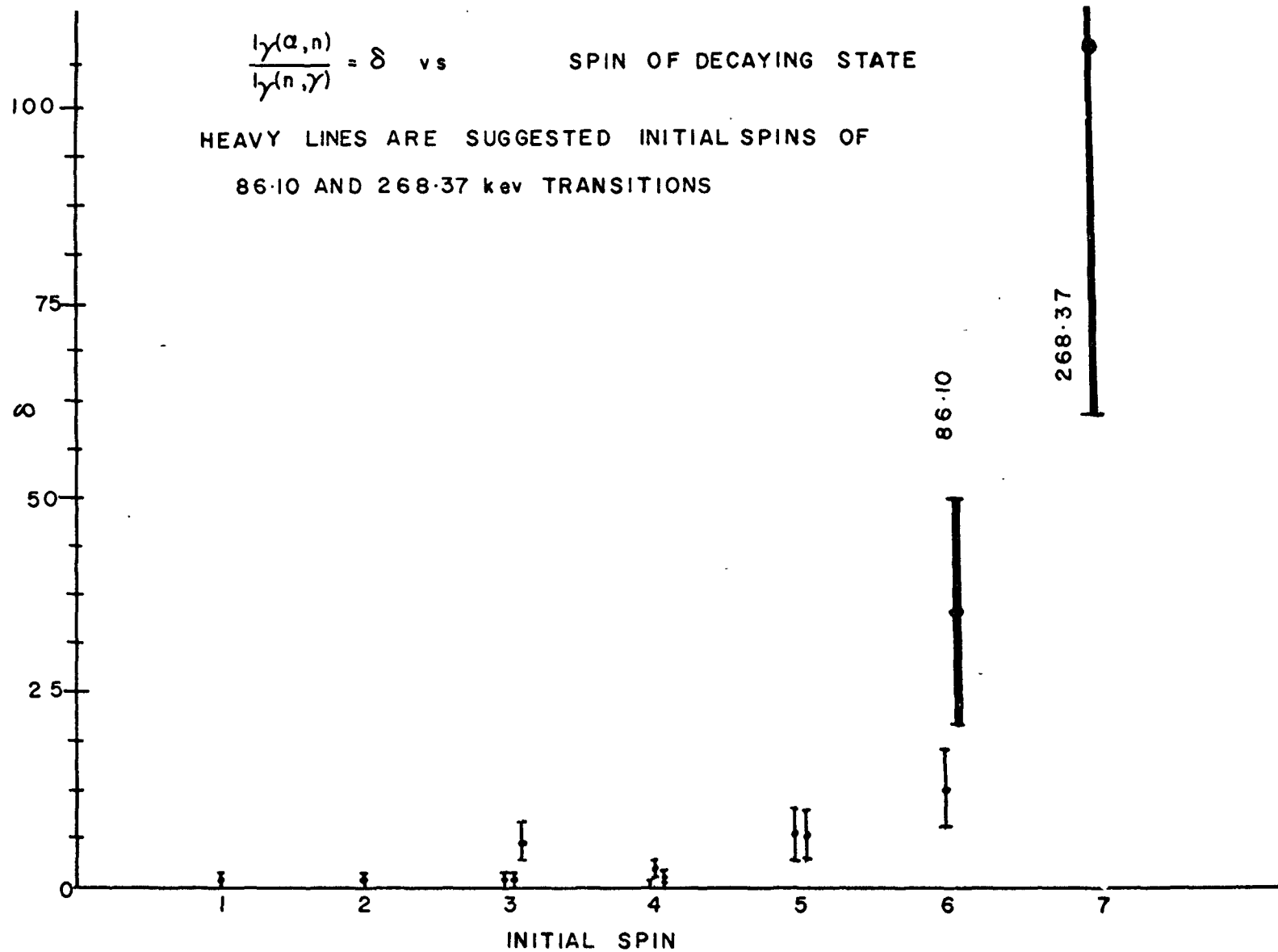
is $5/2^+$, so the capturing state in ^{142}Pr is 2^+ or 3^+.
Consequently these two spins can decay via high energy E1
transitions to states with spin $1^-,2^-,3^-,4^-$. In order to
get to states with spin 5^- or larger, an intermediate
transition between the capturing state and the high spin
state is necessary. On the other hand, in ^{139}La(α,n)
the spin of the ^{139}La ground state is $7/2^+$, and the alpha
particles can themselves bring in large orbital angular
momentum because of their larger mass and momentum.
In Table 6 the dependency of $I_\gamma(\alpha,n)/I_\gamma(n,\gamma)$ is tabulated
as a function of the spin of the decaying state. The
transitions referred to in that table are those depicted in
the level scheme proposed by Kern et al. (Figure 3).
Fig. 12 is the accompanying plot for Table 6. As will be
seen in Figure 12, the points all lie on a smooth curve
except for the point representing the relative increase of
the 159.09(.10) kev transition. According to Kern et al.s'
scheme, the 159.09(.10) and 187.79(.10) kev gammas both
originate from spin 3 states. From the intensity ratios,
it appears, however, that they should both originate from
spin 5 states. This inconsistency is especially glaring
for the 159.09 kev gamma, since this transition is supposed
to originate from the 176.9 kev level. Consequently, the
relative intensity of the 150.09 kev and 176.9 kev gamma
should be constant regardless of the reaction. In (n,γ)
the branching ratio according to Kern et al.(1968) is

$$I_\gamma(159.09)/I_\gamma(176.9) = 1.3/100(30\%) = .013(30\%)$$

but in (α,n), this ratio is

$$I_\gamma(159.09)/I_\gamma(176.9) = 1.6/22.7(40\%) = .069(40\%)$$

Kern et al. report a close doublet 159.11 and 159.33 kev.
We might suppose that the peak area we measured in (α,n)
results from two gammas, and that it is the 159.33 kev

gamma which produces most of the intensity in the doublet. But, if this were the case, it should have been reflected in energy measurement of the doublet since the centroid should have been shifted to the high energy side of the peak. The 159.09 kev transition might ,in fact, come from a high spin state then. Or, there might be another 159.09 kev transition in ^{142}Pr which is not the one that Kern et al. place as originating from the 176.9 kev level. We can not at this moment give a definite explanation for the anomalous intensity of the 159.09 kev gamma in (α,n).

For the 86.10 kev,268.37 kev, and 552.86 kev gammas we note large increases in intensity. In fact , for

86.10 kev	$I_\gamma(\alpha,n)/I_\gamma(n,\gamma)$	=	35(41%)
268.37 kev	$I_\gamma(\alpha,n)/I_\gamma(n,\gamma)$	=	107(47%)
552.86 kev	$I_\gamma(\alpha,n)/I_\gamma(n,\gamma)$	=	essentially infinite

The intensity systematics suggest that all three gammas originate from states with spin greater than 6.

By locating the second 6$^-$ state at 89.739 kev one can account for the large relative increase in the 86.10(.10) kev gamma. The 268.37 kev gamma is not only in coincidence with the 86.10 kev gamma, but also increases its relative intensity one hundred fold from (n,γ) to (α,n). It is suggestive then to assign the level at 358.11(.10) kev a spin of at least 7 to account for the large increase in the intensity of the 268.37 kev gamma. We can assign the level at 358.11 kev as the hitherto missing spin 7$^-$ level, because other possible configurations are not seen this low in excitation energy(at least not in ^{140}La). By assigning this level a spin 7$^-$ we can also account for the 294.48(.10) kev gamma seen in (α,n) as the transition between the level at 358 kev and the one at 64 kev. The closest transition to 294.48 kev seen in

(n,γ) is 294.81 kev(.17)kev, and Kern et al.(1968) believe this to be a transition between levels at 1041.9 and 703.6 kev. In their scheme the 1041.9 kev level is assigned a spin $(2,3)^-$, and from the intensities, if we take the 294.48 and 294.81 kev gammas to be the same gammas, then

$$I\ (\alpha,n)/I\ (n,\gamma)\ =\ 16(51\%).$$

Such a large increase in intensity would suggest an initial spin of 6 at least. The ambiguity can be resolved if we assume that the 294.48 and 294.81 kev gammas are,in fact, two separate transitions. If they were the same the 294.48 kev gamma would be peculiar on two counts, namely

    (a) its intensity behaviour contradicts its
           assignment as a decay from a spin 2 or 3

    (b) it has the largest discrepancy in energy
           between the Kern et al. measurements in $(n\ ,\gamma)$
           and our measurements in 16.5 mev (γ,n).

The peak that we see at 294.48 kev in (α,n) is then a doublet, whose members are separated by $(294.81-294.36)$ = .45(.27) kev. Since the total peak intensity is known to be 11.2(16%) (see Table 3) , if we let I_1 = intensity of 294.36 gamma, and I_2 = intensity of 294.81 gamma, then $I_1 + I_2$ = 11.2, and

$$\frac{294.36 I_1 + 294.81 I_2}{11.2} = 294.48$$

$$= \frac{I_1(294.36) + I_2(294:36+.45)}{11.2} = 294.36 + \frac{I_2(.45)}{11.2}$$

or I_2 = 3 units of intensity. There is quite a large(240%) error on this estimate due to the uncertainties in the gamma energies. Note that from the intensities in (n,γ) in Table 3, one should expect an intensity I_2 no greater than 1 unit. in (α,n).

Figure 13

Suggested Positions of Three New Levels in ^{142}Pr at 89.739(.006)kev, 358.11(.10) kev, and 910.97(.30) kev

THREE NEW NUCLEAR STATES OF
^{142}PRASEODYMIUM

J π EXCITATION (kev)

910·97 (·30)

552·86

268·37

7⁻   358·11 (·10)

294·36

86·056

6⁻   897·39 (·006)

6⁻   63·746

5⁻   3·683

2⁻   0
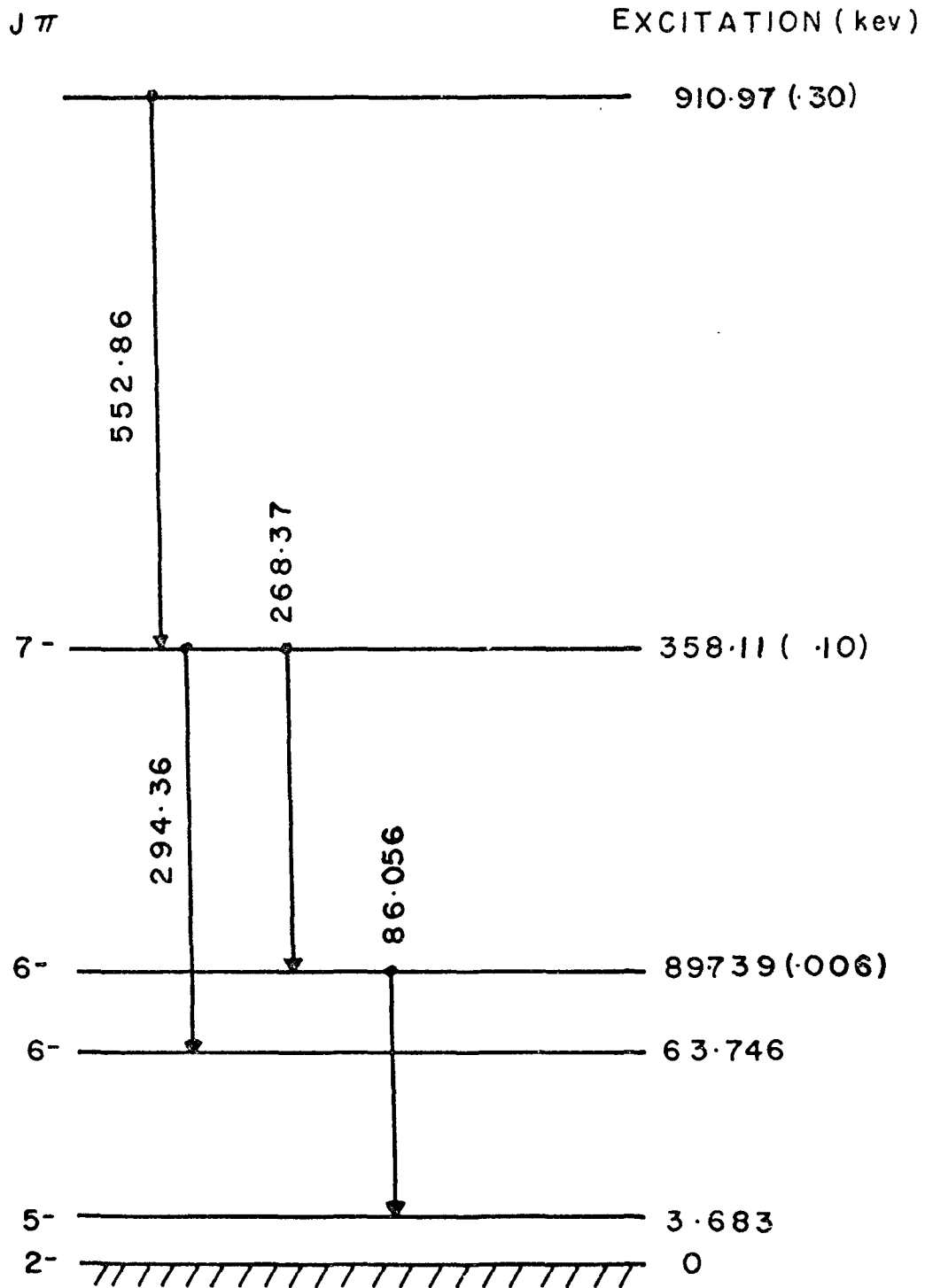
Other evidence for the existence of a level at
358 kev comes from a ^{144}Nd(d,α) experiment conducted by
Macphail. He observed several levels not seen by Kern et al.
(1968), among them a level at 358 kev and a level at 910
kev. Recall, that if we place the 552.86 kev gamma above
the 268.37 kev gamma we obtain a level at 910.97(.30) kev.
Unfortunately the two levels must remain speculative at
the moment because of the low count rate in ^{144}Nd(d,α)
that Macphail encountered.

Relative Level Populations in ^{139}La(α,n) 16.5mev

As mentioned previously, the low lying states can
be described by the mixture of two configurations, namely

$$\left| \tau_1, Jm \right\rangle = \left| \pi^0 2d_{5/2} \nu 2f_{7/2} \; ; \; Jm \right\rangle$$
$$\left| \tau_2, Jm \right\rangle = \left| \pi^0 1g_{7/2} \nu 2f_{7/2} \; ; \; Jm \right\rangle .$$

Kern et al.(1968) assume that transitions within a configuration
are predominantly M1. The rationale behind this assumption
lies in the following:

The transition probability for emission of a photon
of energy $E = \hbar c \kappa$ of multipolarity $\lambda\mu$ and type $\sigma = E$ or M is,

$$T_{if} = \frac{8\pi(\lambda+1)}{\lambda((2\lambda+1)!!)^2} \frac{\kappa^{2\lambda+1}}{\hbar} \left| \left\langle f \left| O^\sigma_{\lambda\mu} \right| i \right\rangle \right|^2$$

where $O^\sigma_{\lambda\mu}$ is a ___ tensor operator of electric or magnetic
type defined by:

electric multipole operator:

$$O_{\lambda\mu} = \sum_i e_i r_i Y^{\mu*}_\lambda(\Omega_i) - ig_{si}\mu_0 \kappa(\lambda+1)^{-1}(\sigma_i \times r_i)\cdot\nabla(r Y^{\mu*}_\lambda)_i$$

magnetic multipole operator:

$$M_{\lambda\mu} = \mu_o \sum_i (g_s \underset{\sim}{S}_i + \frac{2}{\lambda+1} g_{L_i} \underset{\sim}{L}_i) \cdot \nabla (r^\lambda Y_\lambda^{*\mu})_i$$

By making rough estimates for the matrix elements (Preston p.300) one obtains

$$\langle f | Q_{\lambda\mu} | i \rangle \sim ZeR^\lambda \quad \text{R is the nuclear radius}$$

$$\langle f | M_{\lambda\mu} | i \rangle \sim A(e\hbar/2Mc)R^{\lambda-1}$$

The second term in Q is usually neglected because its ratio to the contribution of the first term is on the order of E_γ/Mc^2 , where M is the nucleon mass. However, the second term contributes an amount

$$kA(e\hbar/2Mc)R^\lambda \quad \text{to the matrix element.}$$

Again, following Preston, if ΔJ =0,1, and $\Delta \pi$ = +1, then the ratio of M1 to E2 is on the order of

$$M1/E2 \sim (\hbar/McR)^4 (Mc^2/E_\gamma)^2$$

for ^{142}Pr   R = 7.3 fm, and for an energy E_γ = 300kev,

$$M1/E2 \sim 7$$

An accurate analysis of the transition probabilities involves including the structures of the initial and final states. For example, although an M1 transition satisfies the condition that ΔJ = 0,1, and $\Delta \pi$ = +1, in the single particle model ΔL = 0, that is, the particle in transit must retain its orbital angular momentum. Suppose we have initial and final states for which ΔJ =0,1 and $\pi_i \pi_f$ = 1. Abbreviating the notation we could write

$$\tau_1 = \pi^o 2d_{5/2} \nu 2f_{7/2} \quad , \quad \tau_2 = \pi^o 1g_{7/2} \nu 2f_{7/2}$$

$$|\psi_i\rangle \;=\; d_i\,|\tau_1\rangle \;+\; \beta_i\,|\tau_2\rangle$$

$$|\psi_f\rangle \;=\; d_f\,|\tau_1\rangle \;+\; \beta_f\,|\tau_2\rangle$$

Where the designations E2 and M1 mean that the initial and final states can be connected through their components

$|\tau_1\rangle$ and $|\tau_2\rangle$ by E2 and M1 operators. For M1 transitions the matrix element $\langle\psi_f|\,M1\,|\psi_i\rangle$ will involve a sum of terms (over the 2J + 1 magnetic quantum numbers of the single particle state J) of the form

$$d_f^*\,d_i\,\langle\tau_1|\,M1\,|\tau_1\rangle \;+\; \beta_f^*\,\beta_i\,\langle\tau_2|\,M1\,|\tau_2\rangle$$

that is

$$\langle\psi_f|\,M1\,|\psi_i\rangle \sim \sum_{\substack{m_n\\m_p}} d_f^*d_i\langle\tau_1|M1|\tau_1\rangle + \beta_f^*\,\beta_i\,\langle\tau_2|\,M1\,|\tau_2\rangle$$

We have suggested that the level at 358 kev is the 7^- state described by

$$|7M\rangle \;=\; |\pi^0 1g_{7/2}\,\nu\,2f_{7/2}\rangle$$

This state decays via a 294 kev and a 268 kev transition to levels at 89.7 and 63.7 kev. Since the 268 kev transition is five times as intense as the 294 kev transition, the model we are considering suggests that the level at 89.7 kev has a relatively large component of $\pi^0 1g_{7/2}\,\nu\,2f_{7/2}$ configuration because the M1 transition is favored over an E2 transition since $\Delta L = 0$. We can determine the magnitudes

of the two configurations present in the 89.7 kev and
63.7 kev states by dividing the theoretical transition
rates of the 294 kev and 268 kev gamma and comparing
the ratio to the experimental ratio.

$$\frac{T_{if}(294)}{T_{if}(268)} = \frac{I_\gamma(294)}{I_\gamma(268)} = \left(\frac{294}{268}\right)^3 \left(\frac{\beta(63.7)}{\beta(89.7)}\right)^2$$

$$= \left(\frac{294}{268}\right)^3 \left(\frac{\alpha(89.7)}{\alpha(63.7)}\right)^2 .$$

If we take (see Table 3) $I_\gamma(294)$ = 11.2(16%),
then

$$\frac{I_\gamma(294)}{I_\gamma(268)} = .20(28\%). \text{ Then we have}$$

$$\left(\frac{\alpha(89.7)}{\alpha(63.7)}\right)^2 = .75 \times .20(28\%) = .15 \ (.04)$$

Or, if assume that the 294.48 kev is a doublet, the intensity
of the 294.81 kev gamma should be subtracted from the total
intensity. In this case ($I_\gamma(294.81)$ = 3 units of intensity)

$$\frac{I_\gamma(294)}{I_\gamma(268)} = .15(28\%)$$

And in this case

$$\left(\frac{\alpha(89.7)}{\alpha(63.7)}\right)^2 = .11(.03)$$

Consider now then ^{141}Pr(d,p) data from Hussein. He sees
the level at 89.7 kev with a relative intensity 1.8(.8)
out of 100. The total normalized cross section for two
6^- states is 27.1 . From this information one can again
calculate the ratio of the coefficients discussed above.
The result is

$$\left(\frac{\alpha(89.7)}{\alpha(63.7)}\right)^2 = \frac{1.8(.8)}{27.1-1.8(.8)} = .07 \ (.03)$$

Therefore, within experimental error the coefficients from
the gamma ray studies and the particle transfer study
agree.

If we are correct in believing that these low lying
transitions are predominantly Ml, then the relative population
of the several low lying states in the ^{139}La(α,n)
reaction at 16.5 mev can be determined. This information is
tabulated in Table 7.

The triad of coincident gamma rays in ^{142}Pr is
not unique to this nucleus. Macphail and Summers- Gillreport
that they see similar strong coincidences in ^{144}Pm and
^{146}Eu respectively. In ^{146}Eu the transitions are from
levels 899.8 $\rightarrow$ 274.8 $\rightarrow$ 0 or 651.4 $\rightarrow$ 274.8 $\rightarrow$ 0. Work
done by Macphail reveals a level at 842 kev, and Macphail
believes this to be the initial state of the low energy
multi gamma cascade,however,he believes this level is the
7^- from the $(1g_{7/2},2f_{7/2})$ multiplet.

Neighboring odd Z, even N nuclei,e.g, $_{57}$La^{137},
and ^{139}Pr, have 11/2- spin states at 1.004 mev and .822
mev respectively. This could represent the $1h_{11/2}$ proton
Anticipating that this orbital also exist in ^{142}Pr,
offers the possibility of other configurations besides the
ones involving $2d_{5/2}$ and $1g_{7/2}$. In fact, neighboring even
Z odd N nuclei, for example, ^{143}Nd, (which has a state
at .742 mev and 9/2-) contain the $1h_{9/2}$ neutron orbital.
Consequently , the excitations above 700 kev are possible
mixtures of several configurations, plus coupling of the
shell model states with quadrupole phonons in the core.
The level at 911 kev is therefore, probably not as simple
as the states below 358 kev, but we should expect that it
has a large spin ($j > 5$) since it decays to the 7- state
at 358 kev.

Table 7

Relative Populations of The Low Lying Levels in
^{142}Pr in the 16.5 mev ^{139}La(d,n) Reaction *

Spin	Level(kev)	Intensity
6	63.75	169(23%)
4	72.29	59(26%)
1	84.99	9(20%)
6	89.74	148(21%)
5	128.25	131(34%)
4	144.58	47(26%)
3	176.86	47(35%)
2	200.56	14(17%)
7	358.11	69(13%)
	910.97	21(25%)

* Corrected for internal conversion assuming M1
  transitions.

Summary

The independent quasi particle model for ^{142}Pr successfully describes the gross features of the low lying excitations. The model predicts 14 spin states among the low lying levels. Twelve nuclear states below 358 kev have been discovered, and three of the spin assignments made by Kern et al.(1968) have been corroborated by independent investigators. The other spin assignments by Kern et al. have yet to be confirmed.

The two remaining states of the $(\pi\mathring{1}g_{7/2}\nu 2f_{7/2})$ and $(\pi^{\circ}2d_{5/2}\nu 2f_{7/2})$ configurations, allegedly 0^{-} and 1^{-}, have yet to be located. However, a comparison of the level structure of ^{140}La and ^{142}Pr suggests that the remaining two levels should be found above 358 kev. In ^{140}La the 1^{-} state is at 467 kev and the 0^{-} is at 579 kev. We should expect the 0^{-} and 1^{-} to be roughly in the same energy region for ^{142}Pr. The success of the model and the similarity between the low lying level structures of ^{140}La and ^{142}Pr , encourages one to believe that nuclear structure studies provide a means by which we can gain information about the inter nucleon potential.

References

Amaldi,D'Agostino,Fermi,Rasetti,Segre',Proc Roy Soc, 149A,522(1935)

F.W. Bingham,M.B. Sampson,Phys Rev,128,1796(1962)

G.A. Bartholomew,B.B. Kinsey,Can J Phys,31,1025(1953)

J.M. Cork,R.G. Shreffler,C.M. Fowler,Phys Rev,74,1657(1948)

J.W. deWire,M.L. Pool,J.D. Kurbatov,Phys Rev,61,544(1942)
ibid. (reference B) p.564

R.H. Fulmer,A.L. McCarthy,B.L. Cohen,Phys Rev,128,1302(1962)

L.B. Hughes,T.J. Kennett,W.V. Prestwich,Nucl Phys,89, 241(1966)

S.Hussein, private communication

E.N. Jensen,L.J. Laslett,D.J. Zaffarano,Phys Rev 80,862(1950)

E.T. Jurney,Phys Rev 76,290(1949)

E.T. Jurney,H.T. Motz,S.H. Vegas,Jr.,Nucl Phys A94,351(1967)

J.Kern,G.L. Struble,R.K. Sheline,Bull Am Phys Soc 10, 512(1965)

J. Kern,G. Mauron,B. Michaud,Phys Lett 24B,400(1967)

J. Kern,G.L. Struble,R.K. Sheline,Phys Rev 153,1331(1967)

J. Kern,G.L. Struble,R.K. Sheline,E.T. Jurney,H.R. Koch,
B.P.K. Maier,U. Gruber,O.W.B. Schult,Phys Rev 173,1133(1968)

J. Kern,E.T. Jurney,R.K. Sheline,E.B. Shera,H.R. Koch,
B.P.K. Maier,U. Gruber,H. Baader,D. Breitig,O.W.B. Schult,
G.L. Struble,Phys Rev C 2,2323(1970)

A.M. Lane,NUCLEAR THEORY,W.A. Benjamin Inc,1964,New York,
Amsterdam

M. Macphail, private communication

C.E. Mandeville,Phys Rev 75,1287(1949)

J.K. Marsh,S. Sugden,Nature 136,102(1935)

J. Mellema,F.R. Reddingus,H. Postma,Nucl Phys A157,577(1970)

M.L. Pool,L.L. Quill,Phys Rev 53,437(1938)

M.A. Preston, PHYSICS OF THE NUCLEUS, Addison-Wesley Pub.
Co.,Inc,1962,Reading,Massachusetts,Palo Alto,London

G.L. Struble,Phys Rev 153 ,1347(1967)

R.G. Summers-Gill,private communication